PC1Dmod 6.2

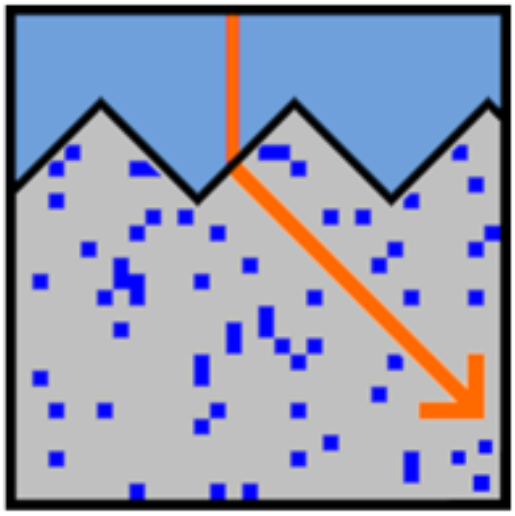

User Manual

Institute for Energy Technology, Norway

Fraunhofer Institute for Solar Energy Systems, Germany

Institute for Energy Technology
Instituttveien 18
NO-2007 Kjeller
Norway
www.ife.no

Fraunhofer Institute for Solar Energy Systems
Heidenhofstr. 2
D-79110 Freiburg
Germany
www.ise.fraunhofer.de

PC1Dmod is an unofficial, modified version of the semiconductor device simulation tool PC1D.
This user guide is provided along with PC1Dmod.
It is based on the help-file of PC1D 5.9.
It is released under the GNU General Public Licence, Version 3 (GPLv3).

Free as in Freedom

The authors, IFE and Fraunhofer ISE make no warranty of any kind, express or implied, with regard to this material.

Date: 2016-04-20

Table of contents

Table of contents 3
1 Program description 5
2 What's new? 6
2.1 What's new in PC1Dmod version 6.2? 6
2.2 What's new in PC1Dmod version 6.1? 6
2.3 What's new in cmd-PC1D version 6.0? 7
2.4 Updates of PC1D version 5.9 and below 7
3 Getting started 8
4 Numerical method 10
4.1 Fundamental equations 10
4.2 Discretization 14
4.3 System solving 16
4.4 Node placement 18
5 Convergence and convergence failure 20
5.1 Dynamic renoding 20
5.2 Situations which are known to interfere with convergence 20
5.3 Improving convergence by controlling the numerical method 21
5.4 Improving convergence by imposing excitation gradually 21
6 Physical models 22
6.1 Refractive index 23
6.2 Optical absorption coefficients 23
6.3 Free-carrier absorption 24
6.4 Reflectance and charge carrier generation 25
6.5 Permittivity 25
6.6 Band structure 26
6.7 Bandgap narrowing 26
6.8 Mobility 27
6.9 Recombination 28
6.10 Incomplete ionization 33
7 Commands 35
7.1 Configuration file 35
7.2 File menu 36
7.3 Device menu 38
7.4 Excitation menu 41

7.5 Compute menu 44
7.6 Graph menu 47
7.7 View menu 48
7.8 Options menu 50
7.9 Help menu 50
7.10 Advanced output options 51
8 Physical constants 52
9 Bibliography 53
9.1 PC1Dmod program development 53
9.2 Physical models included in PC1D version 5.9 53
9.3 Numerical method included in PC1D version 5.9 55
9.4 References added for cmd-PC1D and PC1Dmod 55

1 Program description

PC1Dmod 6.2 is a modification of PC1D, a computer programs written for IBM-compatible personal computers, which solve the fully coupled nonlinear equations for the quasi-one-dimensional transport of electrons and holes in crystalline semiconductor devices, with emphasis on photovoltaic devices.
PC1Dmod 6.2 extends PC1D by (i) including Fermi–Dirac statistics, which can be relevant in regions of high doping, and (ii) adding advanced c-Si models for Auger recombination, band-gap narrowing, and carrier mobility into the well-known graphical user interface of PC1D 5.9. cmd-PC1D adds flexibility through implementing the calculations in a scripting environment.
When selecting the original models, PC1Dmod and cmd-PC1D give the same results as PC1D 5.9. The extensions have been successfully tested against Sentaurus, Edna and/or VBA implementations, but not for all possible scenarios, so use them with care. Please send bugs and suggestions to halvard.haug@gmail.com
All executables can be run on 32-bit and 64-bit Windows. Mac and Linux are not supported.

PC1Dmod is supported and distributed by the Institute for Energy Technology, Norway and the Fraunhofer Institute for Solar Energy Systems, Germany. It is based on PC1D, which has strongly influenced both the PV research and industry for decades. PC1D was written by P.A. Basore, D.A. Clugston *et al.* (see section 9.1). As the program itself, this manual is based on the original PC1D 5.9 help-file.

Only one file is necessary to run the program, PC1Dmod6.2.exe. Several additional files are provided which contain material parameters for selected semiconductors, standardized solar spectra, and example problems. All of the files can be simply copied into the directory of choice; no setup program is required. To store files of different type in different directories, see the instructions for the Options menu.

PC1Dmod will continue to be improved and your suggestions are appreciated. Submit them via e-mail at the address shown above. Of particular interest are any computation errors that may arise, and improved values for material parameters as they become available. Updates of the software will be freely available at pvlighthouse.com.au and at sourceforge.net.

2 What's new?

2.1 What's new in PC1Dmod version 6.2?

(Release date: March 2016).

- Incomplete ionization of several dopants (B, P, As, Ga, and Al) in silicon
- Doping-dependent surface recombination velocity
- Finely resolved solar spectra AM1.5g, AM1.5d and AM0
- Direct calculation of quantities as j_{0e}, $R_{sh,}$ and x_j
- Calculation of fill factor and efficiency, besides voltage and current
- Easy simulation of injection-dependent lifetime curves

Downward compatibility for PC1D 5.9 is still ensured: the parameter files can be used with both tools and PC1Dmod provides the same physical models as PC1D 5.9, additionally to the updated physics.

2.2 What's new in PC1Dmod version 6.1?

(Release date: March 2015).

- The kernel of cmd-PC1D including the physical models is implemented in a modified version of the PC1D 5.9 graphical user interface.
- The bandgap narrowing according to Yan and Cuevas is implemented as alternative to Schenk's parameterization.
- Schindler's extension for compensated silicon of Klaassen's parameterization of the carrier mobility is implemented.
- Specification of new physical models and parameters can now be done using a configuration file, available from the parameter section of the program
- Added an option for setting an external SRH file for position-depending SRH recombination using the configuration file
- Updated parameter section and menus to indicate whenever one of the original models and parameters are not in use
- Increased maximum number of elements per region
- Increased maximum file size and transient lengths
- Increased initial meshing density for external doping profiles
- Updated help section to refer to this file
- Changed colour theme for parameter section and graph

Downward compatibility for PC1D 5.9 is still ensured: the parameter files can be used with both tools and PC1Dmod provides the same physical models as PC1D 5.9, additionally to the updated physics.

2.3 What's new in cmd-PC1D version 6.0?

(Release date: March 2014).
cmd-PC1D is a command-line version of PC1D, thus adding flexibility through implementing the calculations in a scripting environment. The program also introduces several major changes in the device physics. Only a short bullet list is given here, please see section 6 for more details on the physical models.

- Implemented Fermi-Dirac statistics (Now used as default, but Boltzmann statistics can still be used)
- Added new model for band gap narrowing (Schenk 1994)
- Added new model for carrier mobility (Klaassen 1992)
- Added new parameterizations for Auger recombination (Richter *et al.* 2012, Kerr and Cuevas 2002)
- Added updated models for the (temperature dependent) intrinsic carrier density (Altermatt *et al.* 2003) and energy band gap (Green 1990)
- Added new silicon standard value for N_c/N_v ratio, calculated by modifying N_v to match the intrinsic carrier density of silicon

2.4 Updates of PC1D version 5.9 and below

Please see original PC1D help file for change log and updates of previous versions of the PC1D[1].

[1] http://www.sourceforge.net/projects/pc1d/ or http://www.pvlighthouse.com.au/resources/PC1D/help/pc1d_help_index.aspx

3 Getting started

Using PC1Dmod is a three-step process:

1. Set up the simulation parameters. This includes the device and material parameters, and the excitation to be applied to the device.
2. Run the simulation.
3. Examine the results.

PC1Dmod has three different types of displays (called *views*), each useful for a different step of this process.

When setting up the simulation parameters, you will want to use the *Parameter View*. This gives a list of simulation parameters, and a schematic diagram of the device being simulated, giving you visual feedback when parameters are changed. This view also gives a shortcut: you can double-click on any line to bring up a dialog box allowing you change that parameter. You can also double-click on elements of the diagram to change them.

While you run a simulation, you can switch to the *Four-Graph View*. This fills the screen with four graphs of quantities that are commonly of interest (for example, the carrier velocities; generation and recombination; etc). You can watch these quantities change as the program advances in the solution of the problem.

The *Interactive Graph View* is designed for intensive study of a particular graph. It allows you to zoom into regions of the graph which interest you; examine the values of individual points; and copy the graph values to another Windows program (e.g. a spreadsheet) for further analysis.

But, PC1Dmod is designed to flexible! You can switch between views at any time (even while a simulation is running).

If you are just using PC1Dmod or PC1D for the first time, you should take a look at the example parameter files supplied with the program. Spend a little time getting used to the various views, and the methods of changing parameters. A few common questions are answered below.

How do I change the parameters for a simulation?

Either:

- Use the Display menu and Excitation menu; or
- Double-click on the parameters name in the Parameter view (This is the textual list of parameters which you see when you first run PC1Dmod); or
- Double-click on the device schematic to change device parameters. A dialog box will appear, allowing you to specify values for the parameters, which you are interested in.

How do I get PC1Dmod to calculate the results? (How do I run a simulation?)

Either:

- Use the Compute menu and select Run; or
- Press the Run button in the toolbar.

How can I examine the results of a simulation?

1. Switch to interactive graph view. You can do this using the Graph menu.

2. You can zoom into any region of the graph using a mouse or keyboard. Values from the graph can be copied to the clipboard and imported into another program, e.g. a spreadsheet.
3. Or, if you are only interested in the values of V_{oc}, I_{sc}, *FF*, V_{mpp}, I_{mpp}, and P_{max}, they are displayed in the parameter view under the heading *** RESULTS ***

Using the device schematic

A schematic diagram of the device is displayed in the parameter view, providing visual feedback of doping, texturing, and internal shunt elements. This makes it easier to recognize mistakes when designing complex devices. You can also double-click on parts of the diagram to change various parameters.

The parameters, which can be modified from the diagram, are:

Parameter	**Where to click**
Background Doping	Centre of a region
First Front Diffusion	Front 3mm of a region
First Rear Diffusion	Rear 3mm of a region
Front/Rear Texturing	Within 3mm outside the top/bottom of the cell
Surface Charge	Between 3 and 6mm of the top/bottom of the cell
Region Thickness	Within 3mm outside the right of the cell
Shunt elements	Within 3mm outside the left of the cell
Contacts	To the left of the shunt elements

4 Numerical method

This section describes the isolated-element approach used within PC1Dmod to obtain rapid, accurate solutions of the semiconductor transport equations. The emphasis in this program has been on reliable convergence for a broad range of doping profiles and boundary conditions.
The five semiconductor equations (section 4.1) can be readily reduced to three equations in three unknowns. There are several options for selecting the solution variables; none appears to have a significant advantage. For PC1Dmod, we have chosen the electrostatic potential, ψ, and the electron and hole quasi-Fermi potentials, ϕ_n and ϕ_p. Three expressions are required at each interface between elements. Poisson's equation minimizes the total electrostatic energy in the adjoining elements, and both electron and hole currents must be continuous across each interface.

4.1 Fundamental equations

Transport

The numerical method of PC1Dmod uses the two-carrier semiclassical semiconductor transport equations. These equations are derived from the Boltzmann transport equation with the following assumptions:

- the two carriers flow independently (no carrier-carrier scattering),
- both carrier populations remain in thermal equilibrium with the surrounding crystal lattice (no hot carriers),
- the mobility of carriers is isotropic, and
- the structure of the energy levels available to electrons is not significantly affected by excitation (rigid bands, except for injection-dependent bandgap narrowing).

The effect of magnetic fields is also neglected and the device temperature is assumed to be uniform. The resulting equations for electron and hole current density (J_n, J_p) are commonly written in terms of the electron and hole density (n, p), the electron and hole mobility (μ_n, μ_p), and the electron and hole quasi-Fermi energies (E_{Fn}, E_{Fp}).

$$\begin{aligned} J_\mathrm{n} &= \mu_\mathrm{n} \cdot n \cdot \nabla E_\mathrm{Fn} \\ J_\mathrm{p} &= \mu_\mathrm{p} \cdot n \cdot \nabla E_\mathrm{Fp} \end{aligned} \tag{1}$$

Charge carrier statistics

The quasi-Fermi energies relative to their corresponding energy band define which of the energy states available to electrons are filled by carriers from each population, thereby determining the local concentration of both carriers. For non-degenerate material, the Boltzmann exponential approximation to the Fermi-Dirac distribution function can be utilized:

$$\begin{aligned} n &= N_\mathrm{c} \cdot e^{-\frac{(E_\mathrm{c} - E_\mathrm{Fn})}{k_\mathrm{B} \cdot T}} \\ p &= N_\mathrm{v} \cdot e^{-\frac{(E_\mathrm{Ep} - E_\mathrm{V})}{k_\mathrm{B} \cdot T}} \end{aligned} \tag{2}$$

Here N_c and N_v are the effective density of states in the conduction and valence bands. E_c and E_v are the energy levels of the two band edges.

In order to describe degenerate material correctly, Fermi-Dirac statistics are required. For the full Fermi-Dirac calculation however, the carrier densities need to be directly related to the band edges and N_c and N_v through the general expressions

$$\begin{aligned} n &= N_\mathrm{c}\,\mathrm{F}_{1/2}\left(-\frac{E_\mathrm{c}-E_{\mathrm{F}n}}{k_\mathrm{B}T}\right) \\ p &= N_\mathrm{v}\,\mathrm{F}_{1/2}\left(-\frac{E_{\mathrm{F}p}-E_\mathrm{v}}{k_\mathrm{B}T}\right), \end{aligned} \tag{3}$$

$\mathrm{F}_{1/2}$ is the complete Fermi integral of order 1/2, given by

$$\mathrm{F}_{1/2}(\eta) = \frac{2}{\sqrt{\pi}}\int_0^\infty \frac{t^{1/2}}{e^{t-\eta}+1}\,dt. \tag{4}$$

If the quasi-Fermi energies lie within the band gap and are separated from the conduction and valance band edges by more than 0.05 eV, the Boltzmann approximation can be used with negligible error, meaning that $\mathrm{F}_{1/2}(\eta)$ can safely be approximated by an exponential function, and Eq. (3) can be reduced to the form shown in Eq. (2). For very large doping or high injection conditions, the quasi-Fermi energies approach or even merge into the bands, and the semiconductor is said to be degenerate. In these circumstances, the full F-D expressions are needed to obtain correct results.

In PC1Dmod, two different analytical expressions are used to effectively evaluate the F-D operator [12] and it's inverse function [13]. These expressions have previously been shown to lead to less than 0.003% relative error in the carrier concentrations with little loss in computation time [15].

The carrier concentrations in PC1Dmod are then calculated using the same solution variables as in the original PC1D 5.9 program:

$$\begin{aligned} n &= N_\mathrm{c}\,\mathrm{F}_{1/2}\left(\frac{q\psi - q\phi_{n,\mathrm{i}} + \ln\left({n_{\mathrm{i},0}}/{N_\mathrm{c}}\right)}{k_\mathrm{B}T}\right) \\ p &= N_\mathrm{v}\,\mathrm{F}_{1/2}\left(\frac{-q\psi + q\phi_{p,\mathrm{i}} + \ln\left({n_{\mathrm{i},0}}/{N_\mathrm{v}}\right)}{k_\mathrm{B}T}\right), \end{aligned} \tag{5}$$

Note that the terms $\ln(n_{\mathrm{i},0}/N_\mathrm{c})$ and $\ln(n_{\mathrm{i},0}/N_\mathrm{v})$ have been added in the numerator in the expressions for n and p. These terms correspond to $(E_\mathrm{i}-E_\mathrm{c})$ and $(E_\mathrm{i}-E_\mathrm{v})$, respectively, and must be added to account for the change in the energy point of reference when replacing the prefactor $n_{\mathrm{i},0}$ in Eq. (2) with N_c and N_v. The replacement of Eq. (2) with Eq. (5) (as well as the reverse relations) is done throughout the entire PC1D source code. When Boltzmann statistics are chosen by the user the $\mathrm{F}_{1/2}$ function is simply changed to an exponential function (and a natural logarithm for the inverse function). By also selecting the PC1D 5.9 models, this causes the results to revert back to those of PC1D 5.9, as expected.

Define the quasi-Fermi potentials (ϕ_n, ϕ_p) as the separation of the quasi- Fermi energies relative to the equilibrium Fermi energy at some selected reference location. For PC1Dmod, this location is taken as *x=0*. The position of the two band edges in Eq. (2) and (5) relative to this reference energy depends on the electrostatic potential and any spatial variation in the band structure. To describe variations in the band structure, two band-edge potentials are introduced, V_n and V_p. These potentials represent the shift (toward the centre of the bandgap) of the conduction and valence band edges with respect to the conditions at the reference location, after accounting for electrostatic effects. These shifts may be caused by spatial variations in material composition or bandgap narrowing due to heavy doping.

Specifically, for bandgap E_g, electron affinity χ, effective conduction (valence) band density of states N_c (N_v), and conduction (valence) bandgap narrowing ΔE_{gc} (ΔE_{gv}),

$$V_n = \frac{k_B \cdot T}{q} \cdot \ln\left(\frac{N_c}{N_{cr}}\right) + \frac{\chi - \chi_R}{q} + \Delta E_{gc}$$
$$V_p = \frac{k_B \cdot T}{q} \cdot \ln\left(\frac{N_v}{N_{vr}}\right) - \frac{E_g - E_{gR}}{q} + \frac{\chi - \chi_R}{q} + \Delta E_{gv} \tag{6}$$

where q is the magnitude of the elementary electronic charge. The material (conduction and valence band) properties at the reference location can serve to establish a convenient zero reference for the electrostatic potential. Let zero electrostatic potential correspond to neutral intrinsic conditions in this material. Introducing these definitions into Eq. (2) produces a new pair of Boltzmann-like expressions for n and p,

$$n = n_{ir} e^{q(\psi + Vn - \phi_n)/kT}$$
$$p = n_{ir} e^{q(-\psi + Vp + \phi_p)/kT} \tag{7}$$

Here, n_{ir} is the intrinsic carrier concentration at the reference location.
The corresponding equations for Fermi-Dirac statistics read:

$$n = N_c \, F_{1/2}\left(\frac{q\psi + V_n - q\phi_{n,i} + \ln\left({n_{i,0}}/{N_c}\right)}{k_B T}\right)$$
$$p = N_v \, F_{1/2}\left(\frac{-q\psi + V_p + q\phi_{p,i} + \ln\left({n_{i,0}}/{N_v}\right)}{k_B T}\right), \tag{8}$$

Combining Eqs. (1) and (8) it is possible to eliminate n and p, expressing the two unknown current densities in terms of the two unknown quasi-Fermi potentials and the unknown electrostatic potential. All other parameters can be expressed in terms of these unknown quantities for a given device structure, providing two equations for five unknowns.

Continuity equations

Two additional equations can be generated by accounting for the fate of all electrons and holes that enter a given volume of space. These continuity equations account for flow into the volume, creation of carriers within the volume (generation), and annihilation of carriers within the volume (recombination).

$$\frac{\partial n}{\partial t} = \frac{\nabla \bullet J_n}{q} + G_L - U_n$$
$$\frac{\partial p}{\partial t} = \frac{\nabla \bullet J_p}{q} + G_L - U_p \tag{9}$$

Here G_L is the volume generation rate of electron-hole pairs due to the absorption of light (photogeneration), and U_n, U_p are the net volume recombination rates for electrons and holes.
The photogeneration model in PC1Dmod includes a number of sophisticated features, including light trapping and free-carrier absorption. It does not consider the generation of multiple carrier pairs by energetic photons, two-photon absorption processes that use a trap level as an intermediate step, or absorption of photons created during radiative

recombination. PC1Dmod also does not include generation of carriers due to impact ionization, and thus will not predict avalanche breakdown.
A consequence of the two-carrier model is that electrons and holes are always created and annihilated in pairs, so that $U_n = U_p = U$. This approximation is valid only for high-quality material in which the concentration of occupied trap states is small compared with the carrier populations. The net recombination (U) can, in turn, be expressed in terms of the three unknown potentials (ψ, ϕ_n, ϕ_p). The recombination model includes trap-assisted, Auger, and band-to-band processes. Other factors must be neglected for reasons of computational efficiency, including changes in the trap cross-sectional area or energy level as a function of occupation state, and the effect of traps distributed throughout the bandgap.

Poisson's equation

The addition of Eq. (8) makes it possible to eliminate J_n and J_p as unknowns, leaving two equations in the three unknown potentials. Poisson's equation of electrostatics provides the third and final independent equation.

$$\nabla \bullet (\varepsilon \nabla \Psi) = -\rho \qquad (10)$$

where ρ is the volume charge density and ε is the permittivity. Contributions to the charge density include the electron and hole densities and the concentration of ionized donor and acceptor impurities. The two- carrier model neglects the charge associated with trap states located within the bandgap. PC1Dmod assumes that all of the available dopants are ionized. This is an adequate assumption at room temperature and above, especially since the true dopant concentration is rarely known with great accuracy. At lower temperatures, the user must adjust the doping profiles to represent only the ionized dopant density.

Boundary conditions

As with any set of differential equations, boundary conditions represent an essential component in defining a unique solution. For the semiconductor transport equations, three boundary conditions are required at each external surface. A variety of boundary conditions can be used. Most analytical models assume that (i) the majority-carrier concentration is fixed at its equilibrium value, (ii) the minority-carrier concentration is related to the minority-carrier current density by a surface recombination velocity, and (iii) the surface electrostatic potential is shifted from its equilibrium value by an amount equal to the externally-applied voltage. These conditions are appropriate when all surfaces are heavily doped and electrically contacted, either directly or indirectly.
A more general set of boundary conditions is used in PC1Dmod to accommodate lightly doped and insulated surfaces. The three boundary conditions at each surface are based on (i) injected current density, (ii) surface recombination, and (iii) surface electrostatic potential. The injected total current density is zero at insulated surfaces, and is controlled by the external circuit at contacts. PC1Dmod provides two surface recombination models: a Shockley-Read-Hall recombination velocity model that permits separate electron and hole velocities through a trap level located anywhere in the bandgap, and a saturation current density model that gives a recombination rate proportional to the excess *pn* product at the surface. Three boundary conditions are available for the surface electrostatic potential: neutral surface charge density, the surface charge density remains at its equilibrium value, or the surface electric field remains at its equilibrium value. Constant surface charge density is appropriate at metal-semiconductor contacts, including Schottky contacts, whereas constant surface electric field is more appropriate at insulated surfaces.
At electrical contacts, PC1Dmod allows the amount of injected current to be determined, in part, by the device being simulated. A Thevenin-equivalent circuit is attached to each electrical contact, consisting of a voltage source, series resistance, and external shunt elements. By varying the source resistance from a small value to a large value, the entire

spectrum of boundary conditions ranging from fixed-voltage to fixed-current can be simulated.
A complication in applying the injected-current boundary condition arises when the contact itself is not a part of the solution region. It is often the case that a significant distance may lie between the contact and the solution region. Contacts to practical devices are made to heavily-doped material, so one can generally assume that the injected current will enter the solution region as majority-carrier flow spread throughout the region that matches the dopant type at the contact. To simplify matters, PC1Dmod concentrates this majority-carrier current into a single injection point. The resulting electrostatic potential shift at the point of injection presumably causes a similar shift in the electrostatic potential near the contact. There will be a substantial difference, however, if the point of current injection in the solution region is in high-level injection. The difference in injection levels between the solution region and the contact produces an electrostatic potential difference across the intervening material, even when no current is flowing. For this reason, it is better to use the majority-carrier quasi-Fermi potential to determine the voltage at contacts. In the heavily doped material adjacent to the contact, the majority-carrier quasi-Fermi potential must shift in unison with any shift in the electrostatic potential in order to maintain a fixed volume charge density at the surface. Thus, the majority-carrier quasi-Fermi level is a valid indicator of the contact voltage, with the advantage that it does not differ significantly between the solution region and the contact. What difference might exist will be proportional to current and can therefore be modelled using the external series resistance.

4.2 Discretization

The first step in the numerical solution of the semiconductor equations described in Section 4.1 is the discretization of the device, both in time and space. PC1Dmod is a quasi-one-dimensional model, so the device is spatially divided into a finite set of *M* elements along a solution dimension "*x*", which approximately follows the direction of current flow in the device and is not necessarily a straight line. The dividing point between any two elements is called a node. The nodes are numbered from zero at the left boundary to *M* at the right. Subscripts of *j* or *k* are used to denote values at the *jth* or *kth* nodes, respectively. The cross-sectional area for current flow is a function of *x*, with a value A_k assigned to each node.

Poisson's equation

Poisson's equation is satisfied within this discrete space of elements by minimizing the total electrostatic energy of the system, W_e.

$$W_e = \int_0^w \frac{\varepsilon}{2}\left[\frac{\partial \psi}{\partial x}\right]^2 dx - \int_0^w \rho\psi \, dx \qquad (11)$$

where *w* is the width (thickness) of the device. A minimization of this functional with respect to ψ, for a given charge distribution, ρ, gives the electrostatic potential. This minimization is achieved in a discrete sense by approximating ψ, ρ, and e. Both ψ and ρ are given a linear spatial variation within each element. The permittivity, ε, is assumed to be uniform within each element. Setting the differential energy to zero yields the following discrete equation at each internal node *k*:

$$\varepsilon^{-}\frac{A_{k-1}+A_k}{2}\frac{\Delta\psi_{k-1}}{\Delta x_{k-1}} - \varepsilon^{+}\frac{A_{k-1}+A_k}{2}\frac{\Delta\psi_{k-1}}{\Delta x_{k-1}} = \frac{\rho_{k-1}\Delta x_{k-1}A_{k-1}+2\rho_k(\Delta x_{k-1}+\Delta x_k)A_{k-1}+\rho_{k+1}\Delta x_k A_{k+1}}{6} \quad (12)$$

where ε^{+} and ε^{-} refer to the permittivity of the elements on the right and left sides of the node, respectively. In Eq. (12), a delta notation is used to refer to the difference in a value across an element; that is, $\Delta\psi_k = \psi_{k+1} - \psi_k$, and $\Delta\psi_{k-1} = \psi_k - \psi_{k-1}$.

Electron transport

A second discrete equation at each node is based on the transport equation for electrons. Start with a quasi-one-dimensional version of Eq. (1), which gives the electron current, I_n, in the direction of the solution dimension.

$$\mathrm{I_n(x).a_x = -q\,\mu_n(x,E)\,n(x)\,A(x)\,\nabla\phi_n(x)} \quad (13)$$

The denominator of Eq. (13) is assumed to be uniform within each element.
Define a modified electric potential, n(x).

$$\xi_n(x) = \psi(x) + V_n(x) + \frac{kT}{q}\ln\frac{\mu_n(x,E)A(x)}{\mu_r A_r} \quad (14)$$

where μ_r and A_r are arbitrary fixed reference values for mobility and area. Substitute the potentials of Eq. (8) for *n* in Eq. (13) and rewrite the expression in terms of the modified potential of Eq. (14).

$$\mathrm{I_n(x)a_x = -q\mu_r n_{ir} A_r \nabla\phi_n(x)\exp(\frac{q}{kT}[\xi_n(x)-\phi_n(x)])} \quad (15)$$

This equation can be rearranged so that the quasi-Fermi potential is the only position-dependent value on the RHS of the equation.

$$\mathrm{I_n(x)e^{-q\xi_n(x)/kT}a_x = qD_r n_{ir} A_r \nabla e^{-q\phi_n(x)/kT}} \quad (16)$$

where $D_r = \mu_r \cdot kT/q$ defines the reference diffusivity. A contour, or path, integral can be applied to both sides of this equation. The contour is taken across a single element, following the solution dimension *x* from the node at x_k to x_{k+1}.

$$\mathrm{\int_c I_n(x)e^{-q\xi_n(x)/kT}a_x \bullet dl = qD_r n_{ir} A_r \int_c \nabla e^{-q\phi_n(x)/kT} \bullet dl} \quad (17)$$

$$\int_{x_k}^{x_{k+1}} I_n(x)e^{-q\xi_n(x)/kT}dx = qD_r n_{ir} A_r\left[e^{-q\phi_n(x_k)/kT} - e^{-q\phi_n(x_{k+1})/kT}\right] \quad (18)$$

The value of this approach is now apparent. To complete the integration on the LHS of Eq. (18), it is only necessary to make assumptions regarding the spatial variation of two well-behaved variables: I_n and x_n. No assumption regarding the spatial variation of on was necessary. Since the carrier concentration, *n*, depends on both x_n and ϕ_n, this is equivalent to saying that no constraints have been imposed on the spatial variation of *n* within the element. If we assume that both x_n and I_n vary linearly within each element, the integral can be performed to produce a direct expression for the electron current at the left edge of the element (node x_k). Letting β be the inverse thermal voltage, *q/kT*, the following discrete equations for the electron transport result:

$$I_n(x_k) = -\Delta I_n(\beta\,\Delta\xi_n)$$
$$+\ \frac{qD_r n_{ir} A_r}{\Delta x}\Big[\ Z(\beta\,\Delta\xi_n)\exp(\beta(\xi_n(x_{k+1}) - \phi_n(x_{k+1})) - \ Z(-\beta\,\Delta\xi_n)\exp(\beta(\xi_n(x_k) - \phi_n(x_k))\ \Big] \quad (19)$$

where Z(u) = u / (e^u - 1) and Y(u) = (1-Z(u)) /u

In Eq. (19), the net electron current leaving the element, ΔI_n, is equal to the total rate of recombination within the element, minus the total rate of generation, plus the rate that electrons are accumulating as a function of time. In PC1Dmod, photogeneration within each element is based on assuming a separate exponential absorption characteristic for each wavelength, the recombination rate is assumed to vary linearly with position across each element, and carrier accumulation is calculated assuming that the excess electron concentration is a linear function of position. The time dependence of the accumulation is calculated as a backward difference, assuming an exponential function of time unless the excess has changed sign since the last time step, in which case a linear time dependence is used.

Hole transport

A similar derivation as in the previous section gives an expression for hole current, providing the third discrete equation needed at each node.

$$I_p(x_k) = -\Delta I_p Y(-\beta\,\Delta\xi_p)$$
$$-\ \frac{qD_r n_{ir} A_r}{\Delta x}\Big[\ Z(\beta\,\Delta\xi_p)\exp(-\beta(\xi_p(x_{k+1}) - \phi_p(x_{k+1})) - \ Z(-\beta\,\Delta\xi_p)\exp(-\beta(\xi_p(x_k)\ \phi_p(x_k))\ \Big] \quad (20)$$

4.3 System solving

The electron and hole currents at node *k* can each be calculated independently for the two elements that adjoin at that node. Each carrier current should be continuous at the node except for interface recombination and majority-carrier current that may be injected at that node from an external source. Using the discrete expressions for carrier current developed in Section 4.2, two equations at each internal node *k* result.

Hole Current Transport:

$$-\frac{D_r}{\Delta x_{k-1}}\Big[\ Z(-\beta\,\Delta\xi_p)_{k-1}\exp(-\beta(\xi_p - \phi_p)_k) - \ Z(\beta\,\Delta\xi_p)_{k-1}\exp(-\beta(\xi_p - \phi_p)_{k-1})\ \Big]$$
$$+\frac{(\Delta I_p)_{k-1}}{n_{ir} A_r} Y(\beta\,\Delta\xi_p)_{k-1}$$
$$= -\frac{D_r}{\Delta x_k}\Big[\ Z(-\beta\,\Delta\xi_p)_k\exp(-\beta(\xi_p - \phi_p)_{k+1}) - \ Z(\beta\,\Delta\xi_p)_k\exp(-\beta(\xi_p - \phi_p)_k)\ \Big] \quad (21)$$
$$-\frac{(\Delta I_p)_k}{n_{ir} A_r} Y(-\beta\,\Delta\xi_p)_k + \frac{R_s}{n_{ir}} - \frac{I_{maj}}{q n_{ir} A_r}$$

Electron Current Transport:

$$\frac{D_r}{\Delta x_{k-1}}\left[\; Z(\beta\,\Delta\xi_n)_{k-1}\exp(\beta(\xi_n-\phi_n)_k) - Z(-\beta\,\Delta\xi_n)_{k-1}\exp(\beta(\xi_n-\phi_n)_{k-1})\;\right]$$
$$+\;\frac{(\Delta I_n)_{k-1}}{n_{ir}A_r}Y(-\beta\,\Delta\xi_n)_{k-1} \;=$$
$$\frac{D_r}{\Delta x_k}\left[\; Z(\beta\,\Delta\xi_n)_{k}\exp(\beta(\xi_n-\phi_n)_{k+1}) - Z(-\beta\,\Delta\xi_n)_{k}\exp(\beta(\xi_n-\phi_n)_{k})\;\right] \tag{22}$$
$$-\;\frac{(\Delta I_n)_{k}}{n_{ir}A_r}Y(\beta\,\Delta\xi_n)_{k} + \frac{R_s}{n_{ir}} - \frac{I_{maj}}{qn_{ir}A_r}$$

Eqs. (21) and (22), combined with Eq. (12), provide three simultaneous non-linear equations at each internal node. Added to these are three equations at each boundary that are based on (i) injected current density, (ii) surface recombination, and (iii) surface electrostatic potential. The first two of these boundary conditions are implemented using Eqs. (21) and (22), with the expression for current that extends beyond the boundaries of the device set to zero (ie. set LHS to zero at *x*=0). The electrostatic-potential boundary condition either equates the volume charge density at the surface to its equilibrium value (0 for a neutral surface), or equates the electric field at the surface to its equilibrium value. For *M* elements, there are a total of *3(M+1)* equations for *3(M+1)* unknowns.

These non-linear equations are solved using Newton's method, which iteratively solves a sequence of linearized approximations of the equations. A Jacobian matrix is generated using the derivatives of each equation in terms of ϕ_n, ψ, and ϕ_p, each normalized by *kT/q*. The derivatives are calculated from analytical expressions for all terms except the surface and bulk recombination, which are calculated numerically based on a 1% change in the excess carrier densities. These expressions are such that the equations for node *k* involve only values from nodes *k-1*, *k*, and *k+1*. The resulting matrix has a numerical bandwidth of 11. The three equations are ordered so that the matrix will be diagonally dominant, eliminating the need for time-consuming pivoting. The electron current continuity equation is diagonal with ϕ_n, the hole current continuity equation is diagonal with ϕ_p, and the electrostatic equation is diagonal with ψ. A solution vector is constructed using the residual error from the *3(M+1)* system equations. The entries for a single node are shown in Eq. (23).

$$\begin{bmatrix} \frac{\partial f_1}{\partial \phi_n^-} & \frac{\partial f_1}{\partial \psi^-} & \frac{\partial f_1}{\partial \phi_p^-} & \boldsymbol{\frac{\partial f_1}{\partial \phi_n^o}} & \frac{\partial f_1}{\partial \psi^o} & \frac{\partial f_1}{\partial \phi_p^o} & \frac{\partial f_1}{\partial \phi_n^+} & \frac{\partial f_1}{\partial \psi^+} & \frac{\partial f_1}{\partial \phi_p^+} \\ \frac{\partial f_2}{\partial \phi_n^-} & \frac{\partial f_2}{\partial \phi_n^-} & \frac{\partial f_2}{\partial \phi_p^-} & \frac{\partial f_2}{\partial \phi_n^o} & \boldsymbol{\frac{\partial f_2}{\partial \psi^o}} & \frac{\partial f_2}{\partial \phi_p^o} & \frac{\partial f_2}{\partial \phi_n^+} & \frac{\partial f_2}{\partial \psi^+} & \frac{\partial f_2}{\partial \phi_p^+} \\ \frac{\partial f_3}{\partial \phi_n^-} & \frac{\partial f_3}{\partial \phi_n^-} & \frac{\partial f_3}{\partial \phi_p^-} & \frac{\partial f_3}{\partial \phi_n^o} & \frac{\partial f_3}{\partial \psi^o} & \boldsymbol{\frac{\partial f_3}{\partial \phi_p^o}} & \frac{\partial f_3}{\partial \phi_n^+} & \frac{\partial f_3}{\partial \psi^+} & \frac{\partial f_3}{\partial \phi_p^+} \end{bmatrix} \begin{bmatrix} \Delta\phi_n^o \\ \Delta\psi^o \\ \Delta\phi_p^o \end{bmatrix} = -\begin{bmatrix} f_1 \\ f_2 \\ f_3 \end{bmatrix} \tag{23}$$

where superscripts -, o, and + correspond to values at nodes *k-1*, *k*, and *k+1*. The diagonal matrix components are shown in bold characters.

The Jacobian matrix is inverted using LU decomposition. Multiplying the factored Jacobian matrix times the solution vector generates a set of values for $\Delta\phi_n$, $\Delta\psi$, and $\Delta\phi_p$ at each node. The electrostatic potential at each node is then updated using the following function, which puts a clamp on the amount the potential is allowed to change during a single iteration. The clamp value is supplied by the user. The default is *5 kT / q*.

$$\Delta\psi' \;=\; \Delta\psi \;/\; (\,1 + |\,\Delta\psi/\,\text{clamp}\,|\,) \tag{24}$$

The changes in the two quasi-Fermi potentials at each node are also limited, in one of three ways selected by the user. In *Phi* clamping, equation (24) is applied to each quasi-Fermi potential. In *Psi* clamping, the separation between each quasi-Fermi potential and the electrostatic potential is monitored and prevented from changing by more than the clamp value during each iteration, using equation (25). Applying *Both* clamps usually gives the most reliable convergence, through there are exceptions.

$$\Delta\phi' = \Delta\psi' + (\Delta\phi - \Delta\psi') / (1 + |(\Delta\phi - \Delta\psi')/\text{clamp}|) \tag{25}$$

At the end of each Newton iteration, the maximum normalized update (prior to clamping) is determined. The magnitude of this correction is displayed on the screen as a way of monitoring the convergence of the solution. The solution continues until this maximum normalized correction error falls below the user-supplied error limit, typically 10^{-6}.
For equilibrium solutions, the knowledge that $I_n = I_p = G_L = R = 0$ at all x allows the semiconductor equations to be reduced to a single equation in the single unknown, ψ. Thus for equilibrium there are only $M+1$ equations in $M+1$ unknowns, and the numerical bandwidth is reduced to 3. The equations are still quite non-linear, and the same iterative Newton method is applied. At the end of each iteration, ψ is updated, with the clamping function of Eq. (24) applied. The iterations continue until the maximum change in by is less than the user-supplied normalized error limit.

4.4 Node placement

The flexibility of PC1Dmod is greatly enhanced by its ability to automatically place nodes where they are needed most. This "renoding" takes place at various times as requested by the solution parameters. After renoding, the error will usually increase for a few iterations, then converge rapidly toward zero.
The node placement algorithm used in PC1Dmod does not guarantee a specific number of elements. Rather, the user supplies an "Element Size Factor" which directly reflects the intrinsic accuracy of the solution. For the same value of this factor, some problems may require many more elements than others. If more than 500 elements are necessary to achieve the specified level of accuracy, PC1Dmod will automatically increase the element size factor until the number of elements drops below 500. The default value for this factor (a) is 0.5. For more accuracy, consider using a smaller value of a, like 0.25. Values greater than 1.0 provide faster operation, but the solution accuracy will deteriorate.
The node placement algorithm starts with an initial set of elements and proceeds to scan them in order of increasing x. For each element, PC1Dmod chooses one of three options: (i) keep the element as it is, (ii) subdivide the element into up to 30 smaller elements, or (iii) concatenate the element to the element on its left. The determination of which option to take depends on several criteria. These criteria are based on the fundamental assumptions in the numerical method and on producing visually pleasing graphs.
An element will be concatenated to the one on its left unless any of the following tests are true for the two elements combined.

1. The average volume charge density causes the electrostatic potential to deviate from linearity by an excessive amount:

$$\left(\frac{\rho\,\Delta x^2}{2\varepsilon}\right)^{1/2} > \alpha\,\frac{kT}{q} \tag{26}$$

2. The majority-carrier doping concentration changes too rapidly:

$$|\Delta \ln(N_{maj})| > \alpha \tag{27}$$

3. The width of the element is too large for its proximity to the surface (This is to ensure an adequate number of small elements near the front or rear surface in case rapidly absorbed light is subsequently applied):

$$\Delta x > x \tag{28}$$

4. The element consumes too large a fraction of the width of the region:

$$\Delta x > w_{reg}/20. \tag{29}$$

5. The node that would be eliminated by concatenation is the interface between regions or an injection point for the emitter, base, collector, or interface shunt contacts.

The element will be subdivided if either criterion (1) or (4) is true. The number of subelements created will be equal to the ratio of the LHS to the RHS of the equation, with a maximum of 30 subelements permitted.

After a new set of nodes has been selected, the values of the various solution variables at these nodes are obtained by interpolating values from the previous set of nodes. For N_D, N_A, τ_{no}, and τ_{po}, this interpolation assumes that the logarithm of the parameters is linear between nodes; while for ψ, ψ_{eq}, ϕ_n, ϕ_p, A, V_n, V_p, x_n, x_p, v_{sat}, E_t, ε, and G it assumes that the values themselves are linear.

5 Convergence and convergence failure

The equilibrium solution of the semiconductor equations is remarkably robust and will almost always converge. But the extreme nonlinearity of the fully-coupled semiconductor device equations makes convergence to a non-equilibrium solution difficult. Several measures have been taken within PC1Dmod to assist convergence, but despite this, you will eventually generate problems that will not converge. This section offers some advice on how to avoid convergence failure, and how to deal with it when it does occur.

5.1 Dynamic renoding

This feature was introduced in PC1D 4.2, and reduces the likelihood of non-convergence. The basic idea is that when PC1Dmod detects that part of the device is not converging well, it increases the number of finite elements in the difficult area. This helps to ensure that the assumptions, which PC1Dmod makes about the behaviour of solution variables, remain valid.
Dynamic renoding is particularly significant for problems involving reverse biased current sources.
In general, convergence failure occurs either because:

a. the dynamic renoder ran out of nodes (since PC1Dmod 6.1, the limit is 5000) or
b. the solution is trying to reach a final state that is too far removed from the initial state or
c. the situation is unphysical and has no solution.

5.2 Situations which are known to interfere with convergence

The following situations should be avoided as they make convergence difficult:

1. Locating an electrical contact in a region that, in equilibrium, is either very lightly doped or depleted. If the region in equilibrium is clearly of one type or the other, that type will be assumed to be the polarity of the contact, even if subsequent excitation causes the carrier concentrations at that point to become inverted.
2. Connecting a shunt element between two dopant regions that are both isolated by a junction from an electrical contact. This situation occurs in modelling series-connected multijunction devices. It is generally best to model these devices instead as three-terminal devices, then infer the two-terminal behaviour from the three-terminal results.
3. Appling a large forward voltage with no current-limiting resistor. The currents in the device can become huge in this case, and numerical overflow can occur.
4. Low velocity saturation. This is a problem when carriers are trying to go faster than the velocity limit. This problem can be avoided by setting the limit to zero (which disables velocity saturation), or by choosing fixed mobility rather than variable. The problem is even more severe if total velocity saturation is specified for the numerical method.

5.3 Improving convergence by controlling the numerical method

The following actions can be taken to try to get the problem to converge without changing the definition of the problem.

1. Change the element size factor in the Compute: Numerical dialog box.
2. By decreasing the element size factor, you increase the number of elements in the problem. Decreasing this value will tend to improve convergence, until the maximum of 5000 elements is reached. However, the problem will take longer to solve. Sometimes, you will encounter situations where convergence can be improved by *increasing* the element size factor.
3. Adjust the normalized potential clamp (also in the Compute: Numerical dialog box).
4. A smaller value (between 0.1 and 1) will sometimes improve convergence, although some problems benefit from larger clamp values (5-10). It is particularly helpful to reduce this value when voltage, current or light is applied abruptly. Small clamp values increase the time required to solve the problem, especially problems where large reverse-bias voltages are applied.
5. Ensure that *Psi* and *Phi clamping* (in the Compute: Numerical dialog box) are not both disabled.
6. Turn off *Total velocity saturation* (in the Compute: Numerical dialog box) unless you need to include this effect (as you might for some heterostructures where current is limited by velocity saturation in areas of sharp carrier-concentration gradients).
7. On some occasions the difficulty simply may be that the problem converges very slowly. In this case, you should increase the time limit in the Compute: Numerical dialog box.

5.4 Improving convergence by imposing excitation gradually

This is the most effective way of improving convergence. For example, to solve a silicon junction forward-biased to 0.8 volts, you may need to perform an interim solution at 0.6 volts first. You should solve the problem for steady-state at 0.6 volts, then change the bias to 0.8 volts and use Compute: Continue. This will solve for steady-state, using the interim solution as the starting point for the next solution.

Similarly, it may be necessary to increase the light intensity in steps, say 10 mW/cm², 100 mW/cm², then 1 W/cm².

If you have a particular interest in understanding exactly why a particular problem did not converge, you can enable *Graphs after every iteration* in the Compute:Numerical dialog, and create a user-defined graph of *Convergence Error* (plotted on a log scale) versus *Distance from front*. This will show how far each element of the device is from convergence.

6 Physical models

A list of the recommended models that have been implemented in PC1Dmod with focus on crystalline silicon is presented in Table 1. The models have been selected with much care and to best knowledge of the authors. However, Table 1 does not necessarily represent a final, fully correct and consistent set of models for simulation of siicon solar cells. For instance there are still issues with carrier mobility in heavily doped material, as Schenk's BGN parameterization and experimental data for compensated Si were not available when Klaassen published his mobility parameterization. Another open question is the choice of BGN. Very recently, Yan and Cuevas presented an empirical parameterization of BGN for highly *n*-type doped Si [3], in which the authors state that their experimental findings are not compatible with Schenk's widely accepted BGN model.

Table. 1. The full set of recommended models with focus on crystalline silicon that currently are implemented into the PC1Dmod program, together with the numerical approximations for the Fermi operator and it's reverse.
** As default, these models are evaluated at each iteration to account for high injection effects. There is also an option to evaluate these models only for equilibrium conditions in the beginning of the simulation, with the advantage of a slightly higher computation speed.*

Model	Symbol	Ref.	
Intrinsic carrier density	$n_{\mathrm{i},0}$	Altermatt *et al.* 2003	[1]
Intrinsic energy band gap	$E_{\mathrm{g},0}$	Green 1990	[2]
Effective density of states, conduction band	N_{c}	Green 1990	[2]
Effective density of states, valence band	N_{v}	(adjusted to match $n_{\mathrm{i},0}$)	
Bandgap narrowing	$\Delta E_{\mathrm{c}}, \Delta E_{\mathrm{v}}$	Schenk 1998* or Yan and Cuevas 2013 Yan and Cuevas 2014	[3] [4] [5]
Carrier mobility	μ_n, μ_p	Klaassen 1992* Schindler *et al.* 2014	[6, 7] [8]
Intrinsic recombination	U_{intr}	Richter *et al.* 2012 Kerr and Cuevas 2002	[9] [10]
Dopant ionization	N_A^-/N_A	Altermatt 2006 (I+II) (with data from;)	[11, 12] [13, 14]
Numerical approximations for:			
Fermi integral	$u = \mathrm{F}_{1/2}(\eta)$	Van Halen and Pulfrey 1985	[15]
Inverse Fermi integral	$\eta = f_{1/2}(u)$	Antia 1993	[13]

6.1 Refractive index

The index of refraction can be either a fixed value or a function of wavelength using data imported from an external disk file. External index-of-refraction files are standard ASCII files with a filename suffix INR. Each line in the file should contain two numerical values, separated by one or more spaces or a tab. The first value on each line is a value of free-space wavelength, in nm. The second value on each line is the index of refraction at that wavelength. The maximum number of lines allowed is 1000. All values of the index must be positive, and the values of wavelength must increase monotonically. If the range of wavelengths provided is less than is required for the solution of a problem, the index of refraction for the first (or last) wavelength is used for all smaller (or larger) wavelengths.
For crystalline silicon, the refractive index published by Martin Green in 2008 [16] is provided in a file along with the main program.

6.2 Optical absorption coefficients

The optical absorption coefficient as a function of wavelength can be generated as a function of temperature using an internal model, or read from an external disk file. When experimental data for the temperature of interest is available, it is generally better to use this data than to rely on the internal model. Only absorption that leads to photogenerated carriers should be considered, since PC1Dmod assumes that every intrinsically absorbed photon produces an electron-hole pair. Parasitic absorption processes can be modelled through the Free-Carrier Absorption dialog.

Internal model

The internal model for photon absorption includes two direct-gap transitions and eight indirect transitions. The indirect transitions are based on two indirect gaps and either absorption or creation of phonons having two possible energies. Temperature affects the absorption coefficient, a, through a decrease in the energy gaps and through a change in the probability of phonon-assisted transitions. The entries required in the absorption dialog are the energy gaps at 300 K. All four energy gaps are assumed to depend on the absolute temperature (T) through a temperature coefficient (β) and temperature offset (γ):

$$E_G = E_{Go} - \frac{\beta\, T^2}{T + \gamma}. \tag{30}$$

The contributions to the absorption coefficient due to direct transitions for photons with energy $h \cdot \nu$ greater than the energy gap E_{Gdi} are given by

$$\alpha_{di} = A_{di}\sqrt{h\nu - E_{Gdi}}; \quad i = 1,2. \tag{31}$$

The eight phonon-assisted transitions for indirect-gap energies E_{Gi} and phonon energies E_{pj} take the form

$$\alpha_{ij\pm} = A_{ij}\frac{\left(h\nu - E_{Gi} \pm E_{pj}\right)^2}{\pm\left(e^{\pm E_{pj}/kT} - 1\right)}; \quad i = 1,2;\ j = 1,2. \tag{32}$$

The upper signs correspond to phonon-absorbing transitions, while the lower signs are for phonon-creating transitions. Only those terms for which $h\nu \pm E_{pj} > E_{Gi}$ are included. Otherwise, there is no absorption due to that transition. The indirect-gap absorption is clamped for energies greater than the next-higher direct gap. All ten absorption coefficients are added together to yield the total absorption coefficient for each incident wavelength of light ($h\nu = hc/\lambda$, where hc = 1239.84193 eV·nm).

External absorption files

External absorption files are standard ASCII files with a filename suffix ABS. Each line in the file should contain two numerical values, separated by one or more spaces or a tab. The first value on each line is a value of free-space wavelength, in nm. The second value on each line is the absorption coefficient, in cm^{-1}. The maximum number of lines allowed is 1000 (increased from 200 in PC1D v5.9 and below). . All values of the absorption coefficient must be positive, and the values of wavelength must increase monotonically. If the range of wavelengths provided is less than is required for the solution of a problem, the absorption coefficient for the first (or last) wavelength is used for all smaller (or larger) wavelengths. For this reason, it is important that the last entry in the file give an absorption coefficient of zero. Otherwise, PC1Dmod will assume that the final (nonzero) value applies even out to very long wavelengths, thereby greatly overestimating the total photogeneration. Room-temperature absorption files are provided with PC1Dmod for several materials, including crystalline silicon at 300 K [16].

6.3 Free-carrier absorption

Free-carrier absorption competes with intrinsic absorption, reducing the fraction of photons, which generate electron-hole pairs.
The free-carrier absorption across a device is not only dependent upon the wavelength of incident light, but also depends upon the profile of the carrier concentrations across the device. It can be specified by the free-carrier absorption coefficient, which for monochromatic incident light is assumed to take the form

$$\alpha_{FC} = K_1 n \lambda^a + K_2 p \lambda^b \tag{33}$$

where K_1, K_2, a, b are empirically determined constants, n and p are measured in cm^{-3}, α in 1/cm and λ in nm. In PC1D 5.9, estimates of these parameters were available for several materials, see Table 1.

Table 1: Coefficients for free-carrier absorption in selected materials

Material	K_1	a	K_2	b	Source
AlSb	1.9×10^{-24}	2			Fan [17]
GaAs	4×10^{-29}	3			Fan [17]
GaP	(1.5×10^{-24})	(1.8)			Fan [17]
GaSb	9×10^{-31}	3.5			Fan [17]
Ge	~5×10^{-25}	~2			Fan [17]
InAs	6.5×10^{-29}	3			Fan [17]
InP	5×10^{-27}	2.5			Fan [17]
InSb	2.8×10^{-25}	2			Fan [17]
Si	2.85×10^{-26}	2.6	1.64×10^{-25}	2.4	Rüdiger *et al.* [18]

Si	1.16×10^{-26}	2.88	9.89×10^{-25}	2.18	Baker-Finch *et al.* [19]
Si	2.6×10^{-27}	3	2.7×10^{-24}	2	Schmid [20] and Green [21]

For reasons of speed, PC1Dmod calculates the photogeneration only once for each solution step, using the values of *n* and *p* which were calculated for the previous step. For example, the steady-state photogeneration will be based on the equilibrium concentrations of electrons and holes. Although *n* and *p* will vary from their equilibrium values, the perturbation is unlikely to have a significant effect.
For the rare situations where the change in *n* and *p* during solution is important, the Compute:Continue menu command can be used at the conclusion of a steady-state problem. This will cause the photogeneration to be recalculated, using the values of *n* and *p* obtained from the steady-state solution. The steady state solution will then be resolved using the new photogeneration.

6.4 Reflectance and charge carrier generation

The optical model of PC1Dmod is simple and fast, but is not as accurate as advanced ray tracing simulations.
The external front and rear surface reflection can either be calculated internally from the refractive indices and thicknesses of thin films and the substrate applying Fresnel's equations or can be defined by a data file containing the wavelength in nm in the first column and the corresponding reflectance in the second column, separated by white space.
The internal reflection at the rear and the front surface are calculated internally assuming either specular or diffuse reflection. The amount of reflection can be specified by the user.
The absorption within the substrate is assumed to obey the Lamber-Beer law. Absorption in the substrate can occur (a) by exciting electrons from the valence to the conduction band, i.e. by band-to-band absorption, which leads to the generation of one electron-hole pair and (b) by exciting electrons or holes within their respective bands, i.e. by free-carrier absorption, without generating mobile charge carriers.
The optical model is described in more detail in Ref. [22, 23].

6.5 Permittivity

This is the low-frequency (dc) value of the relative permittivity ε_r, expressed as a multiple of the permittivity of free space. This value is also known as the dielectric constant of the material. It defines the amount of charge needed to produce a given electric field in the material.
The value of ε_r for silicon is roughly 12.

6.6 Band structure

The “Device:Materal:Band Structure” command opens a dialog box which contains several parameters that are intrinsic to the band structure of the material.
In the original PC1D program, the band gap is used with the electron affinity to establish the location of the conduction and valence band edges relative to the vacuum level. The N_c/N_v ratio refers to the effective density of states for the conduction and valence bands. This ratio affects the location of the intrinsic energy level within the bandgap. When using Boltzmann statistics, the band gap and N_c/N_v ratio does not influence the solution[2], but they become important when using F-D statistics. Note that E_g, N_c and N_v cannot all be set independently to ensure that they are always consistent with the selected value for the intrinsic carrier density n_i.
The value of the intrinsic carrier density n_i has a major impact on the results obtained for any minority-carrier device. In the original PC1D model, three values can be entered for the intrinsic carrier concentration, at 200, 300 and 400 K. These values are used to interpolate a value for the solution temperature, using a parabolic fit of log(n_i) versus 1/T. In PC1Dmod a new temperature dependent model for n_i is used as default, using the latest value of $n_i = 9.65 \cdot 10^9$ cm^{-3} for silicon at 300 K [17]. Users may also manually set constant values for n_i, E_g and the N_c/N_v ratio in the configuration file (section 7.1).

6.7 Bandgap narrowing

PC1Dmod offers different models for bandgap narrowing:

1. Schenk’s comprehensive theoretical model for crystalline silicon
2. The model by Yan and Cuevas derived from experiments for crystalline silicon
3. The simple model by Del Alamo and Swanson for Boltzmann statistics, used in PC1D 5.9

The models (including the third option for bandgap narrowing) used in PC1D 5.9 and earlier versions were developed for use together with Boltzmann statistics, and should therefore be re-evaluated when changing to Fermi-Dirac statistics. This is particularly true for bandgap narrowing (BGN), as the models used in PC1D 5.9 represent the *apparent* BGN, which account for various effects, including degeneracy at high doping levels. Because of this, Fermi-Dirac statistics should not be applied together with the *apparent* BGN models, as this would overestimate the high doping effects. In case of Fermi-Dirac statistics, the model by Schenk or by Yan and Cuevas should be applied. At the time of writing, discussions are going on, which of the two models is more accurate. While Schenk’s theoretical model is widely used and accepted, the experimental findings of Yan and Cuevas support their parameterization, but are incompatible with Schenk’s.
In PC1Dmod, the user can choose to evaluate the BGN at every iteration step (tends to be more accurate) or only once (tends to be faster).
You can switch between the different models using the configuration file (section 7.1).

[2] In the original PC1D program, the band gap and Nc/Nv ratio was of importance for calculating heterostructures, as the affect the discontinuity at the band edges at interfaces between different regions. In order to implement F-D statistics in PC1Dmod, all band structure parameters have been defined globally for the entire device, meaning that simulations of heterojunction structures are no longer possible. This has been done for practical reasons and will hopefully be fixed in a future update of the program.

Schenk BGN

Schenk developed a comprehensive theoretical model for both *p*- and *n*-type Si [3], which is derived for the case of Fermi-Dirac statistics from a non-self-consistent, full random phase approximation formalism, taking both carrier–carrier and carrier–dopant interactions into account. The bandgap narrowing according to Schenk therefore depends on the carrier and the doping densities, and the temperature.

In its implementation in PC1Dmod as in PC1D 5.9, the total BGN, i.e. the sum of the shifts of the valence ΔE_v and of the conduction bands ΔE_v, is applied to one of the band edges only, according to the doping polarity of the material. In the space charge region the local equilibrium carrier densities are used as input to the Schenk model in order to avoid excessively large BGN values in this region.

For the equations describing the model, the reader is referred to Schenk's paper [3].

Yan and Cuevas BGN

Very recently, Yan and Cuevas presented an empirical parameterization of BGN for highly *n*-type phosphorus-doped Si [4] and highly *p*-type boron-doped Si [5]. The BGN is parameterized as function of dopant concentration. The authors state that their experimental findings are not compatible with Schenk's widely accepted BGN model.

The equations describing the BGN according to Yan and Cuevas can be found in the literature [4, 5].

Del Alamo-Swanson BGN

This is the model was presented by del Alamo and Swanson [24] and is implemented in PC1D 5.9. It is recommended to use this model with Boltzmann statistics since it describes *apparent* BGN. The parameters entered for bandgap narrowing allow the equilibrium *pn* product to depend on the local doping density according to the following expression:

$$\begin{aligned} pn &= n_{ie}^2 = n_i^2 e^{(\Delta E_c + \Delta E_v)/kT}, \\ \Delta E_c &= Slope_N \times \ln\left(\frac{N_D}{Onset_N}\right), \\ \Delta E_v &= Slope_P \times \ln\left(\frac{N_A}{Onset_P}\right), \end{aligned} \tag{34}$$

where the log expressions are taken equal to zero for doping densities less than the respective onset values.

6.8 Mobility

The mobilities of electrons and holes can either be set to fixed values throughout the region, or calculated based on the temperature and local carrier and doping density using one of the following models.

In PC1Dmod, you can switch between these model using the configuration file (section 7.1).

Klaassen-Schindler mobility

This is a model specific to silicon. It is comprehensive, describing the mobilities of electrons and holes as both majority and minority carriers as function of dopant and carrier concentration and of temperature. Klaassen's work for uncompensated silicon [6, 7] was

extended for compensated silicon recently by Schindler *et al.* [8]. Due to their complexity, the reader is referred to the original works for the relevant equations and parameters.

Caughey-Thomas mobility

This mobility model was implemented in PC1D 5.9. It is based on a publication by Caughey and Thomas [25]. Arora *et al.* included the temperature dependence [26]. The model uses a different set of coefficients where the carrier is in the minority than where it is in the majority. The expression used has the following form:

$$\mu(x,T) = \mu_{\min} T_n^{\beta 1} + \frac{(\mu_{\max} - \mu_{\min}) T_n^{\beta 2}}{1 + \left(\frac{N_D(x) + N_A(x)}{N_{ref} T_n^{\beta 3}} \right)^{\alpha T_n^{\beta 4}}}, \tag{35}$$

where T_n is the temperature normalized to 300 K. The mobility model also allows for a maximum velocity for each carrier. This is implemented as a reduction in the mobility at each point in the device where the velocity that the carriers would have achieved approaches or exceeds the saturation velocity. The low-field mobility is replaced with a high-field mobility given by:

$$\mu_{HF} = \frac{\mu_{LF}}{\sqrt{1 + \left(\mu_{LF} E / v_{sat} \right)^2}}. \tag{36}$$

Normally, the electric field is used for "*E*". This produces the required mobility reduction in regions where the high carrier velocity is due to a high electric field, as at junctions. A more accurate approach is to use the gradient in the quasi-Fermi potential in place of E in this expression. This can be done in PC1Dmod by selecting *Total velocity saturation* in the Compute:Numerical dialog box. Note, however, that convergence is less robust and solutions will take much longer with this option selected.
The mobility model does not account for mobility degradation due to carrier-carrier scattering associated with high-level injection.

6.9 Recombination

Intrinsic recombination refers to e.g. Auger and radiative recombination, i.e. recombination that is influenced by temperature, doping, and electric field. These parameters are often fairly consistent for a given material, and thus are included as material parameters. In contrast, the Shockley-Read hall recombination rates for surfaces and bulk are not considered to be an intrinsic property of the material, and are set separately for each region.

Intrinsic recombination

In PC1Dmod, there are three options for intrinsic recombination:

- Auger and radiative recombination in silicon according to Richter *et al.* [9]
- Auger recombination in silicon according to Kerr and Cuevas [10]
- Auger and radiative recombination as in PC1D 5.9

You can switch between these models using the configuration file (see section 7.1).

Richter et al.

The newest and widely accepted parameterization of Auger recombination in silicon was published by Richter *et al.* in 2012 [9]. It was developed for both *p*- and *n*-type silicon, and for low and high injection conditions at 300 K. Coulomb-enhancement is included. Injection-dependent radiative recombination is accurately described.
The radiative recombination rate is parameterized as

$$R_{\mathrm{rad}} = \left(n \cdot p - n_{\mathrm{i,eff}}^2\right) \cdot B_{\mathrm{rel}} \cdot B_{\mathrm{low}} \tag{37}$$

with the electron and hole concentrations n and p, the effective intrinsic density $n_{\mathrm{i,eff}}$, the coefficient $B_{\mathrm{low}} = 4.73\times10^{-15}\,\mathrm{cm^3/s}$ valid for low-injection conditions, and the injection-dependent coefficient [27]

$$B_{\mathrm{rel}} = b_{\mathrm{min}} + \frac{b_{\mathrm{max}} - b_{\mathrm{min}}}{1 + \left(\frac{n+p}{2b_1}\right)^{b_2} + \left(\frac{n+p}{2b_3}\right)^{b_4}}, \tag{38}$$

where

$$\begin{aligned} b_{\mathrm{min}} &= r_{\mathrm{max}} + \frac{r_{\mathrm{min}} - r_{\mathrm{max}}}{1 + \left(\frac{T}{r_1}\right)^{r_2}}, \\ b_1 &= s_{\mathrm{max}} + \frac{s_{\mathrm{min}} - s_{\mathrm{max}}}{1 + \left(\frac{T}{s_1}\right)^{s_2}}, \\ b_3 &= w_{\mathrm{max}} + \frac{w_{\mathrm{min}} - w_{\mathrm{max}}}{1 + \left(\frac{T}{w_1}\right)^{w_2}}. \end{aligned} \tag{39}$$

Please note that compared to the original publication, where an error occurred, b_1 and b_3 are corrected here to $2b_1$ and $2b_3$ respectively. The numerical values of the parameters are given in Table 2

Table 2: Parameters and numerical values for the parameterization of the injection-dependent radiative recombination [27].

b_{max} =	1.00			b_2 =	0.54	b_4 =	1.25
r_{max} =	0.20	r_{min} =	0.00	r_1 =	320	r_2 =	2.50
s_{max} =	1.5×10^{18}	s_{min} =	1×10^{7}	s_1 =	550	s_2 =	3.00
w_{max} =	4.0×10^{18}	w_{min} =	1×10^{9}	w_1 =	365	w_2 =	3.54

The combined Auger and radiative recombination rate is parameterized as

$$\begin{aligned} R_{\mathrm{Auger}} = (n \cdot p - n_{\mathrm{i,eff}}^2) \cdot (&2.5 \cdot 10^{-31} g_{\mathrm{eeh}} \cdot n_0 + 8.5 \cdot 10^{-32} g_{\mathrm{ehh}} \cdot p_0 + 3 \cdot 10^{-29} \Delta n^{0.92} \\ &+ B_{\mathrm{rel}} \cdot B_{\mathrm{low}}). \end{aligned} \tag{40}$$

with the enhancement factors

$$\begin{aligned} g_{\mathrm{eeh}}(n_0) &= 1 + 13\left\{1 - \tanh\left[\left(\frac{n_0}{N_{0,eeh}}\right)^{0.66}\right]\right\} \\ g_{\mathrm{ehh}}(p_0) &= 1 + 7.5\left\{1 - \tanh\left[\left(\frac{p_0}{N_{0,ehh}}\right)^{0.63}\right]\right\} \end{aligned} \tag{41}$$

and $N_{0,\mathrm{eeh}} = 3.3\times10^{17}\ \mathrm{cm^{-3}}$ and $N_{0,\mathrm{eeh}} = 7.0\times10^{17}\ \mathrm{cm^{-3}}$.

Kerr and Cuevas

This parameterization for Auger recombination in silicon published in 2002 [10] was developed for arbitrary injection level and arbitrary doping at 300 K. Compared to free-

particle Auger-recombination, the recombination rate enhancement due to Coulomb attraction of electrons and holes is included. The recombination rate reads

$$R_{\text{Auger}} = n \cdot p \cdot (1.8 \cdot 10^{-24} n_0^{0.65} + 6 \cdot 10^{-25} p_0^{0.65} + 3 \cdot 10^{-27} \Delta n^{0.8}). \quad (42)$$

Since Kerr and Cuevas don't give any units and normalization constants, the equation is only valid if the equilibrium electron and hole concentrations n_0 and p_0, the excess carrier concentration Δn, and the electron and hole concentrations n and p all are inserted in units of cm^{-3}, an R_{Auger} is then given in $cm^{-3}s^{-1}$.
This parameterization is consistent with a constant coefficient $B = 9.5 \cdot 10^{-15} cm^3/s$ of the radiative recombination rate $R_{rad} = B \cdot n \cdot p$.

PC1D 5.9

Within this approach, three Auger recombination coefficients are required to properly compute recombination in either heavily doped or highly injected material. The n-type and p-type coefficients apply to material in low-level injection, while the high-injection coefficient applies to material in high-level injection. The high-injection coefficient represents the sum of both n-type and p-type Auger recombination. It is included as a single factor because in high-level injection the excess electron and hole concentrations are similar. The recombination rate due to Auger processes is computed from the following expression, which weights the result to favor either the low-injection or high-injection coefficients as appropriate:

$$\begin{aligned} R &= \left(C_n n + C_p p\right)\left(pn - n_{ie}^2\right), \\ C_n &= C_{nLLI}\left(\frac{N_D}{N_D + p}\right) + \frac{C_{HLI}}{2}\left(\frac{p}{N_D + p}\right), \\ C_p &= C_{pLLI}\left(\frac{N_A}{N_A + n}\right) + \frac{C_{HLI}}{2}\left(\frac{n}{N_A + n}\right). \end{aligned} \quad (43)$$

A band-to-band recombination coefficient can be provided. This is primarily important only for direct-bandgap materials. The additional recombination at each point due to coefficient B is given by

$$R = B\left(pn - n_{ie}^2\right). \quad (44)$$

Field-enhanced recombination

The Hurkx model for trap-assisted tunnelling [28] is used. This extends the conventional SRH recombination expression to include trap-assisted tunneling enhanced by the local electric field. This model replaces the carrier lifetimes τ_n and τ_p in the SRH model with $\frac{\tau_n}{1+\Gamma}, \frac{\tau_p}{1+\Gamma}$ where Γ is defined by:

$$\Gamma = prefactor.\frac{|F|}{F_\Gamma} \exp\left[\left(\frac{F}{F_\Gamma}\right)^2\right] \quad (45)$$

This expression can be parametrised by specifying a prefactor ($prefactor = 2\sqrt{3\pi} \cong 6.14$) and the value of F_Γ at 300K. Hurkx gives:

$$F_\Gamma = \frac{\sqrt{24 m^* (kT)^3}}{q\hbar} \quad (46)$$

and suggests $m^* = 0.25 m_0$.

WARNING: Do not use this model blindly!
This model is only valid provided the electric field does not get too large. It will be valid in general for midgap traps, but for shallow traps in regions of very high electric field, it may dramatically overestimate the impact of trap-assisted tunneling (for high fields, Γ no longer depends exponentially on F). In these situations, the value for the prefactor and for F_Γ can be modified to give more realistic simulations.
At present, there is insufficient experimental data to justify a more complex model, although Hurkx provides an additional high-field equation (eqn A5 of Ref. [28]).

Shockley-Read-Hall bulk recombination

The bulk recombination model used by PC1Dmod supplies a single Shockley-Read-Hall (SRH) energy level with separate electron and hole lifetimes and an adjustable trap energy level within the bandgap*. The dialog box for specifying these parameters for the current region can also be opened using a button on the toolbar.* This toolbar button will appear to be depressed if the electron or hole lifetime has been altered from its default value of 1 ms.

$$R_{SRH} = \frac{pn - n_{ie}^2}{\tau_n\left(p + n_{ie}e^{-E_t/kT}\right) + \tau_p\left(n + n_{ie}e^{E_t/kT}\right)}. \tag{47}$$

The trap level, E_t, is specified with respect to the intrinsic level, which lies near the middle of the bandgap. The electron and hole lifetimes specified at the top of the dialog box are the values corresponding to intrinsic material at a temperature of 300 K.
Also listed in the bulk-recombination dialog box is the excess-carrier lifetime in low-level injection and the corresponding diffusion length, for material with the background doping and reference temperature specified in the dialog box. These calculated values include the effect of band-to-band and Auger recombination, the coefficients for which are specified for the material's band structure in this region, and also the effects of background doping on the SRH lifetimes as specified in the material recombination dialog. To obtain a specific low-level-injection lifetime or diffusion length, simply type the desired number in the space provided. PC1Dmod will calculate the intrinsic electron and hole lifetimes needed. Note that the properties of the material (band-to-band, Auger recombination, etc.) place an upper limit on the achievable lifetime and diffusion length for a given background doping density.
If an external SRH file for position-dependent SRH recombination is used, it will override the values for τ_n, τ_p set in the recombination dialog. The file should have no headers and three columns: [x in µm], [τ_n in s] and [τ_p in s]. If max(x) < total device thickness, the last entry is used for the rest of the device. Note that the external file is specified for the entire device and not for each region.
Parameters can be entered for the material to indicate the effect of temperature and doping on SRH surface and bulk recombination. For bulk lifetime, the values of τ_{n0} and τ_{p0} specified for the region are modified for use in the SRH recombination formula to reflect the actual device temperature and the local doping density. These parameters can be adjusted to either increase or decrease the impact of temperature and doping. The temperature effect is given by the following formula, applied to both electron and hole lifetimes:

$$\tau(T) = \tau_o\left(\frac{T}{300\text{K}}\right)^\alpha, \tag{48}$$

and the doping effect is given by

$$\tau(N) = \tau_o\left(\frac{N}{N_{onset}}\right)^\alpha; \quad N > N_{onset} \tag{49}$$

The parameters in these two expressions are empirical and very dependent on the crystal growth technology. For silicon, reasonable choices are -0.5 for the temperature exponent, -0.4 for the doping exponent, and 10^{15} cm^{-3} for the onset.

Shockley-Read-Hall front/rear surface recombination

The surface recombination model used by PC1Dmod supplies a single Shockley-Read-Hall (SRH) energy level with separate electron and hole lifetimes and an adjustable trap energy level within the bandgap. *The dialog box for specifying these parameters for the front or rear surface of the current region can also be opened using buttons on the toolbar.* These toolbar buttons will appear to be depressed if there is recombination at that surface. When either S_n or S_p is nonzero, the SRH surface recombination rate is given by

$$R_S = \frac{S_n S_p \left(pn - n_{ie}^2 \right)}{S_p \left(p + n_{ie} e^{-E_t/kT} \right) + S_n \left(n + n_{ie} e^{E_t/kT} \right)}. \tag{50}$$

The trap level, E_t, is specified with respect to the intrinsic level, which lies near the middle of the bandgap. The electron and hole surface recombination velocities specified at the top of the dialog box are the values corresponding to intrinsic material at the reference temperature specified in the dialog box. The values of S_n and S_p entered are modified for use in the recombination formula to reflect the actual device temperature and the surface doping density. The extent of this modification depends on the parameters listed in the material recombination dialog box.

Also listed in the surface-recombination dialog box is the effective minority-carrier surface recombination velocity for material with the surface doping at a temperature of 300 K. To obtain a specific minority-carrier surface recombination velocity, simply type the desired number in the space provided. PC1Dmod will calculate the intrinsic electron and hole surface recombination velocities needed.

For surface recombination velocities, both electron and hole values are modified using the following formulas, which have the same form as the bulk-lifetime expressions.

$$S(T) = S_o \left(\frac{T}{300\text{K}} \right)^{\alpha}, \tag{51}$$

and the surface doping effect is given by

$$S(N) = S_o \left(\frac{N}{N_{onset}} \right)^{\alpha}; \quad N > N_{onset} \tag{52}$$

The parameters in these two expressions are very dependent on the surface treatment process. For thermal oxide on n-type silicon, reasonable choices are 0.5 for the temperature exponent, 1.0 for the doping exponent, and 10^{18} cm^{-3} for the onset. Further parameterizations are given in Ref. [29]. No consistent dependence of S on surface doping density has been demonstrated for p-type silicon at the time of this writing.

Since PC1Dmod version 6.2, another doping-dependent model for the surface recombination velocity is available, which allows setting the front and rear recombination velocity parameters S_n and S_p as a function of the surface doping concentration using the parameterization given in Ref. [29]

$$\begin{aligned} S_\mathrm{p} &= S_{p1} \cdot \left(\frac{N}{N_\mathrm{p1}} \right)^{\gamma_\mathrm{p1}} + S_\mathrm{p2} \cdot \left(\frac{N}{N_\mathrm{p2}} \right)^{\gamma_\mathrm{p2}} \\ S_\mathrm{n} &= S_\mathrm{n1} \cdot \left(\frac{N}{N_\mathrm{n1}} \right)^{\gamma_\mathrm{n1}} + S_\mathrm{n2} \cdot \left(\frac{N}{N_\mathrm{n2}} \right)^{\gamma_\mathrm{n2}}. \end{aligned} \tag{53}$$

In highly-doped silicon, PC1Dmod sets the majority carrier recombination parameter to 10^7 cm/s and the minority carrier recombination parameter to the value according to the parameterization. Values for the parameters for Si:P can be found e.g. in [15].
When high-level injection occurs at the surface, you can choose to either continue with the Shockley-Read-Hall model (the "S" model), or you can choose instead to maintain the saturation current density at the surface at the same value it had in low-level injection:

$$J_o = \frac{qS_nS_p}{S_p\left(p_{eq} + n_{ie}e^{-E_t/kT}\right) + S_n\left(n_{eq} + n_{ie}e^{E_t/kT}\right)}. \tag{54}$$

The choice of high-level-injection model for surface recombination has no effect when the surface remains in low-level injection.

Important Note on Surface Recombination
When there is more than one region in the device, the front and back surfaces refer to the current region, not the device as a whole. The recombination rate calculated for the back surface of region 1 is added to the recombination rate calculated for the front surface of region 2 to get the total rate of recombination at the interface between the two regions.

6.10 Incomplete ionization

The performance of crystalline silicon (c-Si) devices is greatly influenced by the equilibrium carrier concentrations of electrons (n_0) and holes (p_0), both in the base and in highly doped regions like solar cell emitters or back surface fields (BSFs). For uncompensated *p*-type Si p_0 is normally set to be equal to the acceptor dopant density N_A, thus assuming that all dopants are ionized. However, when the Fermi level E_F is close to the dopant energy level E_dop, a significant fraction of the dopant levels are occupied, and the resulting incomplete ionization (i.i.) should therefore often be taken into account. In PC1Dmod 6.2 the well-accepted model for i.i. published by Altermatt *et al.* in 2006 [11, 12] is implemented, which is based on a combination of theory and experimental data for P, B and As from the literature. It is worth noting that this i.i. is not describing the fraction of electrically active dopants in substitutional lattice sites, and is therefore not used to describe e.g. dopant activation of high concentrations of phosphorus and the solubility limit of dopant atoms in Si.
For a correct quantification of i.i., E_dop needs to be known as a function of the doping density N_dop, as E_dop approaches the band edge at high doping levels due to the so-called metal-insulator transition, leading to almost complete ionization at the highest dopant densities [11].
For the device implementation in PC1Dmod 6.2, we have chosen to use the recommended set of simplified equations assuming a discrete dopant energy level, given in Ref.[12]. The fraction of ionized dopants is then described as a function of the carrier densities n and p instead of the Fermi level, simplifying the computation:

$$\frac{N_\mathrm{D}^+}{N_\mathrm{D}} = 1 - \frac{b \cdot n}{n + g \cdot n_1}, \qquad \frac{N_\mathrm{A}^-}{N_\mathrm{A}} = 1 - \frac{b \cdot p}{p + g \cdot p_1}. \tag{55}$$

Here, g is the degeneracy factor ($1/2$ for donor levels and $1/4$ for acceptor levels) and the parameter b depends on N_dop as

$$b = \frac{1}{1 + \left(N_\mathrm{dop}/N_\mathrm{b}\right)^d}. \tag{56}$$

n_1 and p_1 are statistical factors determined by E_dop

$$n_1 = N_\mathrm{C} \exp\left(-\frac{E_\mathrm{dop}}{kT}\right), \quad p_1 = N_\mathrm{V} \exp\left(-\frac{E_\mathrm{dop}}{kT}\right), \tag{57}$$

which in turn is a function of N_dop, parameterized as

$$E_\mathrm{dop} = \frac{E_\mathrm{dop,0}}{1 + \left(N_\mathrm{dop}/N_\mathrm{ref}\right)^c}. \tag{58}$$

The i.i of each type of dopant is thus described by the six parameters $E_\mathrm{dop,0}$, N_ref, c, N_b, d and g, which have been adapted to give the best description of experimental data in each case. These parameters are listed in Table 3 for five common dopants. In addition to P, B and As, which were investigated in Ref. [11, 12], we have also included recently published values for Al [13] and Ga [14]. For the device simulation the user can specify whether i.i. should be included and which dopants to use through the configuration file (see section 7.1). Several iterations of the calculation are performed for the equilibrium case in order to reach a consistent set of values which satisfy both charge neutrality $p + N_D^+ = n + N_A^-$ and the law of mass action $pn = n_\mathrm{i}^2$. The i.i. calculation is also performed at each iteration, thus also taking into account the effect of excess carriers. Note that Al and Ga both have rather high values for $E_{dop,0}$, and the degree of i.i. is therefore more pronounced for these dopants. When simulating the Al-BSF it has been shown that i.i. has a significant effect on the simulated saturation current density $J_{0,p+}$ of these regions [13, 30]. For the case of Ga dopants, it should be noted that Ref. [14] only provides values for $E_\mathrm{dop,0}$, N_ref, c and g and therefore only specifies the behavior of the curve up to the insulator-metal transition, that is before the turning point where the fraction of ionized dopants starts to increase towards unity at the highest doping levels. In order to avoid the unphysical behavior of a monotonically decreasing fraction of ionized Ga dopants at higher N_dop the values for boron-doped silicon (Si:B) may probably be used for N_b and d, but users should be warned that i.i. calculations for Ga above this level will be less accurate.

Table 3. List of parameters used to describe i.i. of various dopants in c-Si

Dopant		Si:P	Si:As	Si:B	Si:Al	Si:Ga
Ref.		[12]	[12]	[12]	[13]	[14]
$E_\mathrm{dop,0}$	(meV)	45.5	53.7	44.39	69.0	72.0
N_ref	(cm^{-3})	3×10^{18}	4×10^{18}	1.7×10^{18}	5.4×10^{18}	5×10^{18}
c		2	1.5	1.4	3	0.75
N_b	(cm^{-3})	6×10^{18}	1.4×10^{19}	6×10^{18}	5.5×10^{18}	*
d		2.3	3	2.4	2.6	*
g		½	½	¼	¼	¼

*Parameters not used in Ref. [14], and they are therefore here set equal to the values for Si:B. These parameters mainly affect the i.i. above the metal insulator transition $N_A \approx 10^{18}$ cm^{-3}, and results using Ga dopants are therefore highly uncertain at high dopant concentrations above this level.

7 Commands

7.1 Configuration file

In order to have a parameter file (*.prm) that is fully compatible with PC1D 5.9 and to select and configure the physical models newly implemented in cmdPC1D 6.0 and PC1Dmod 6.1, a configuration file (*.cfg) is introduced in PC1Dmod 6.1. If the parameter-file is opened with PC1D 5.9, the models introduced in a later version are not available. The configuration file is used to specify selected models and parameters. The configuration file syntax is as follows:

```
Keyword1        name_1a
Keyword2        name_2b
Parameter1 =    value_1;
Parameter2 =    value_2;
```

A complete list of all keywords, parameters and available options is given in Table 4

Table 4: keywords and options for the configuration file.

Keyword	Option	Description	
Carrier statistics	FD	Fermi-Dirac statistics	Default
	Boltzmann	Boltzmann statistics	
Band Gap	Green1990	Intrinsic band gap according to [2]	Default
	PC1D5	n_i as implemented in PC1D 5.9	
DOS Ratio	Haug2014	N_c/N_v ratio adjusted, [31]	Default
	PC1D5	N_c/N_v as in PC1D 5.9	
BGN	Eq_Schenk1998	Band gap narrowing according to [3] evaluated at equilibrium only	
	Schenk1998	BGN according to [3] evaluated at every iteration step	Default
	YanCuevas2014	BGN according to [4, 5]	
	PC1D5	BGN according to [24], as in PC1D 5.9	
Mobility	Eq_Klaassen1992	Carrier mobility according to [6, 7] evaluated at equilibrium only	
	Klaassen1992	μ according to [6, 7] evaluated at every iteration step	Default
	Eq_Schindler2014	μ according to [8] evaluated at equilibrium only	
	Schindler2014	μ according to [8] evaluated at every iteration step	
	PC1D5	μ according to [25, 26], as in PC1D 5.9	
Intrinsic Recombination	Richter2012	Auger and radiative recombination according to [9]	Default
	KerrCuevas2002	Auger recombination according to [10]	
	PC1D5	Intrinsic recombination as in PC1D 5.9, see graphical user interface	

Incomplete Ionization	PC1D5	100% dopant ionization	Default
	Altermatt2006 P+B	Dopant ionization according to [11, 12]	
	P+Ga	Ga data from [14]	
	P+Al	Al data from [13]	
	As+B		
	As+Ga		
	As+Al		
ni =	Value;	Manually set the intrinsic carrier concentration in cm^{-3}	
Eg =	Value;	Manually set the intrinsic band gap in eV	
NcNv =	Value;	Manually set the N_c/N_v ratio	
External_SRH_File =	"filename.txt"	Read in external file specifying position-dependent Shockley-Read-Hall parameters*	
Front SRV parameters =	S01 Nref1 gamma1 S02 Nref2 gamma2;	Front SRV parameterization according to [29]	

*The external Shockley-Read-Hall file should be placed in same folder as the parameter file. The file should have no headers and three columns: [x in µm], [tau0n in s] and [tau0p in s]. If max(x) < total thickness, the last entry is used for the rest of the device.

7.2 File menu

The File menu offers the following commands:

- Description Enter or modify a text description of the contents of this parameter file.
- New Creates a new parameter file.
- Open Opens an existing parameter file.
- Close Closes an opened parameter file.
- Save Saves an opened parameter file using the same file name.
- Save As Saves an opened parameter file to a specified file name.
- Print Prints the current window.
- Print Preview Displays the current window on the screen as it would appear printed.
- Print Setup Selects a printer and printer connection.
- Exit Exits PC1Dmod.

New

Use this command to create a new parameter file in PC1Dmod.
You can open an existing parameter file with the Open command.

Shortcuts

Toolbar:
Keys:CTRL+N

Open

Use this command to open an existing parameter file. The parameters for a problem, including a description of both the device and excitation, are stored in a binary-encoded parameter file with a PRM suffix. The parameter file also specifies external data files that

may be necessary to describe parameters that are a function of position, wavelength, or time.
You can create new parameter files with the New command.
Shortcuts
Toolbar:
Keys:CTRL+O

Close
Use this command to close all windows containing the active parameter file. PC1D suggests that you save changes to your parameter file before you close it. If you close a parameter file without saving, you lose all changes made since the last time you saved it. Before closing an untitled parameter file, PC1Dmod displays the Save As dialog box and suggests that you name and save the parameter file.

Save
Use this command to save the active parameter file to its current name and directory. When you save a parameter file for the first time, PC1D displays the Save As dialog box so you can name your parameter file. If you want to change the name and directory of an existing parameter file before you save it, choose the Save As command. The parameters for a problem, including a description of both the device and excitation, are stored in a binary-encoded file with a PRM suffix. The parameter file also specifies external data files that may be necessary to describe parameters that are a function of position, wavelength, or time.
Shortcuts
Toolbar:
Keys:CTRL+S

Save as
Use this command to save and name the active parameter file. PC1Dmod displays the Save As dialog box so you can name your parameter file.
To save a parameter file with its existing name and directory, use the Save command.

Print
Use this command to print the current window. This command presents a Print dialog box, where you may specify the range of pages to be printed, the number of copies, the destination printer, and other printer setup options.
Shortcuts
Toolbar:
Keys:CTRL+P

Print preview
Use this command to display the active current window as it would appear when printed. When you choose this command, the main window will be replaced with a print preview window in which one or two pages will be displayed in their printed format. The print preview toolbar offers you options to view either one or two pages at a time; move back and forth through the current window; zoom in and out of pages; and initiate a print job.

Print setup
Use this command to select a printer and a printer connection. This command presents a Print Setup dialog box, where you specify the printer and its connection

Exit

Use this command to end your PC1Dmod session. You can also use the Close command on the application Control menu. PC1Dmod prompts you to save parameter files with unsaved changes.

Shortcuts

Mouse: Double-click the application's Control menu button.
Keys:ALT+F4

7.3 Device menu

The Device menu offers selections in four groups:

Region manager	This group of selections allow you to manipulate the number of regions in your device. Each region can be a different material, with its own parameters.
Region Parameters	This group of selections pertain only to the current region. They allow you to examine and modify the thickness, material, doping, and recombination parameters.
Device Parameters	This group of selections pertains to the device as a whole. They allow you to examine and modify the area of the device, surface texture, surface charge, external circuit contact locations, and the optical reflectance, both external and internal.
Device Files	This group of commands (New, Open, SaveAs) allows you to create, retrieve, and store device files, having a suffix DEV. These contain all of the information about the device only, with no excitation or numerical solution data. Since PC1Dmod 6.1, additional data is stored in the configuration file and the SRH file, with the DEV file being completely downward compatible to PC1D 5.9.

Region manager

The Region Manager selections in the Device Menu offer the following commands:

Select Region	Selecting a region number makes that the “current” region, such that any examination or modification of region parameters using the Device Menu will apply to that region. A region can also be selected by clicking on any line pertaining to that region in the Parameter View. *The current region is displayed on the toolbar as a button. Pressing this button increments the current region.* Region numbers that are not defined for this device are disabled.
Insert Region	Selecting a number inserts a new region at that point in the device. Region 1 is always the front of the device. The new region will be defined with parameters that duplicate the most recently selected region, except that surface recombination and diffusions are set to zero. Once inserted, the new region becomes the current region.
Remove Region	Selecting a number removes that region from the device. Any higher-numbered regions are shifted toward the front of the device. The current region is reset to one of the regions still remaining.

Region parameters

The Region Parameter selections in the Device menu allow you to examine or modify the parameters in the following categories. In each case, the command applies only to the region that is currently selected. *The currently selected region is indicated on the toolbar as a button.*

Thickness

This command opens a dialog box for specifying the thickness of the current region, in units of µm.

Material

In the material section, important material properties can be set. Since PC1Dmod 6.1, this is not always used. If you specify models in the configuration-file that are different from the ones used in PC1D 5.9, this section is not only partly applied!
The parameters that define a type of material can be stored in binary files having the suffix MAT. Three commands at the bottom of the Material menu allow you to create, retrieve, and store these material files. Several MAT files for the most commonly encountered materials are provided with PC1Dmod. Loading a new MAT file will only affect the current region. In addition, the Material menu allows you to examine and modify the following parameters for the current region: Permittivity, Band Structure, Material Recombination, Field-Enhanced Recombination, Bandgap Narrowing, Mobilities, Refractive Index, Optical Absorption Coefficients, Free-Carrier Absorption.

Doping

This selection allows you to specify the doping densities for donors and acceptors in the current region.

Background doping

This command opens a dialog box where you can specify the doping density and the doping type (n-type or p-type) for background doping that is present uniformly throughout the layer. The mobilities at 300 K for both electrons and holes at this doping density are displayed for reference, as are the diffusivities. The mobilities are either fixed or variable with doping, as selected for this region's material). The majority-carrier mobility shown is used to calculate the resistivity. If you want the doping density that corresponds to some desired 300-K resistivity, then you can just type the desired resistivity directly into this field, then hit the Tab key to set the doping density accordingly.

Front/Rear diffusions

Doping profiles can be specified for both the front and rear surfaces of the current region. These profiles can be generated using internal models or can be imported from an external disk file.
The internal model allows for two diffusions at each surface. After selecting either the first or second diffusion for the surface, a dialog box is opened for specifying the diffusion details. *The dialog box for the first diffusion on the front and rear surfaces can also be opened using a button on the toolbar.* Each diffusion must be enabled within its dialog box before it becomes active. The toolbar button will appear to be depressed if that diffusion has been enabled. Diffusions can be specified as n-type or p-type. Each diffusion can take one of four shapes, defined as follows:

Uniform $$N(x) = N_o; \quad x_p < x < x_p + x_d$$

Exponential $$N(x) = N_o e^{-|x - x_p| / x_d}$$

Gaussian $$N(x) = N_o e^{-\left(x-x_p\right)^2 / x_d^2}$$

Erfc $$N(x) = N_o \operatorname{erfc}\left((x - x_p) / x_d\right)$$

where N_o is the Peak Doping, x_d is the Depth Factor, and x_p is the Peak Position, all of which are adjustable. Note that $N(x) = N_o$ for $x<x_p$ for the Erfc shape.
Also shown in the dialog box are the calculated sheet resistance (Ω/sq) and junction depth. The junction depth is based on the currently specified background doping density for the region. The sheet resistance is calculated based on the diffusion profile up to this junction depth, using a temperature of 300 K and the majority-carrier mobility (either fixed or variable, as specified for this region's material). The calculation of the sheet resistance ignores conductance due to dopants from the background or from other diffusions.
To obtain a diffusion with a given junction depth and sheet resistance, you can type the desired sheet resistance in the space provided, then press the Tab key. The Peak Doping is adjusted to give the requested sheet resistance. If the junction depth does not match the desired value, type the desired value in that field, then press Tab to adjust the Depth Factor to obtain the desired junction depth. If the sheet resistance is affected, you can re-enter the desired value in that space, and repeat the cycle until convergence is obtained. Rarely are more than a few iterations required to get quite close to the desired combination.
External diffusion profiles are standard ASCII files with a filename suffix DOP. These can be created using a text editor or generated by another computer program. Each line in the file should contain three numeric values, each separated by one or more spaces or a tab. The first value on each line is a value of distance inward from the surface of the region, with units of mm. The second value on each line is the donor doping density at that position, with units of cm-3. The third value on each line is the acceptor doping density, with units of cm-3. The position values must start at 0 and increase monotonically. The maximum number of positions that may be defined in the file is 500.

Recombination
This selection allows you to specify the recombination parameters in the bulk and at both the front and rear surface of the region. Bulk Recombination, Front/Rear Surface Recombination

Thickness
This command opens a dialog box for specifying the thickness of the current region, in units of µm.

Device parameters
This group of selections pertains to the device as a whole. They allow you to examine and modify the area of the device, surface texture, surface charge, external circuit contact locations, and the optical reflectance, both external and internal.

Device files
This group of commands (New, Open, SaveAs) allows you to create, retrieve, and store device files, having a suffix DEV. These contain all of the information about the device only, with no external doping profile, excitation or numerical solution data.

7.4 Excitation menu

The excitation menu offers the following commands:

Mode	This command opens a dialog box which allows you to control whether excitation is applied, and if so, whether it is steady-state or transient.
Temperature	This command opens a dialog box which allows you to set the temperature of the device. You can specify the temperature in either kelvin or degrees Celsius. This temperature is also used to compute adjustments to the carrier mobilities, bulk and surface recombination, optical bsorption, the exponential factor for any internal shunt diodes, etc.
Base/Collector Source Circuits	These commands open dialog boxes which allow you to specify the Thevinin-equivalent circuits for the base and collector. These circuits are only active if base and/or collector contacts have been enabled for this device.
Photogeneration	This selection allows you to introduce photogeneration in the device. Illumination can be provided from a primary and/or secondary light source, or the photogeneration profile can be supplied from an external file.
Excitation Files	This set of commands (New, Open, SaveAs) allows you to create, retrieve, or store binary files that contain all of the parameters needed to define the excitation. These excitation files, with suffix .exc, can then be used with a variety of different devices. Since version 5.0, the graph definitions are also saved in the excitation files.

Excitation Mode (Excitation menu)

The excitation mode line can be set to Equilibrium, Steady State, or Transient. The choice determines the final state the solution will achieve before stopping. The solution will always proceed by solving first for Equilibrium, then Steady State, then Transient. If the Mode is Transient, it is necessary to supply additional details for controlling the time dependence of the solution. The Step Size is the elapsed time between time steps. Setting this value too small may cause convergence problems. Large values (e.g. 1 second or more) can be used to simulate the quasi-static response of the device to a swept excitation. Examples include current versus voltage and spectral response versus wavelength. The initial time step, which immediately precedes t=0, can be set to a different value from the remaining steps. Setting this value small permits the simulation of an abrupt change in excitation at time t=0. The entry for Number of Time Steps is the number of time steps of duration Time Step Size that are desired. The total duration of the transient will be the product of these two values.

Base/Collector Source Circuit (Excitation menu)

There are two identical Thevinin-equivalent source circuits; one associated with the base contact and one associated with the collector contact. Both circuits contain a voltage source and a series resistance. Different values of voltage and resistance can be specified for steady state versus transient conditions. Changing the voltage between its steady-state and initial transient value causes a step change in voltage at $t = 0$. Setting the final transient value different from the initial transient value causes the voltage to sweep linearly from the initial to the final value during the course of the transient solution. The source series resistance affects how much current flows in the device for a given source voltage, but the loss associated with these elements is not reflected in the device performance as revealed in plots of collector or base current versus voltage. The value of series resistance can be specified either in Ω, or in Ωcm. In the latter case, the series resistance is adjusted for each solution based on the area of the device being simulated. A constant-voltage condition at a

contact is achieved by setting the corresponding source series resistance to zero. A constant-current condition is maintained by setting both the source voltage and series resistance to large values, so that their ratio gives the desired current. The open-circuit voltage at either the collector or base contact can be obtained by setting the source voltage to a small (can be zero) value, and the corresponding resistance to a large value (1 MΩ is usually plenty). When a simple linear voltage ramp is not adequate, time-dependent source-voltage values can be supplied from an external ASCII data file having a filename with suffix ".VLT". Each line in the file should contain three numerical values, separated by one or spaces or by a tab. The first value on each line should be the time (in seconds), the second value is the source voltage (in V), and the third value should be the series resistance (in Ω).The time values must be monotonically increasing. The maximum number of lines read from the file is 1000 (increased from 200 in version 5.9). Note that the time values in this file do not affect the time steps used in the solution, which are determined by the Mode command. Rather, voltage values for each time step are interpolated from this file.

Photogeneration (Excitation menu)

The photogeneration options allow you to apply photoexcitation to the device, either as a photogeneration profile supplied via an external file, or using one or both of two light sources which can illuminate either the front or rear surface of the device. When using the light sources, PC1Dmod internally calculates the photogeneration rate within the device. At each incident wavelength, after accounting for incident-surface reflection, the light is absorbed in the device using the absorption coefficients for each region. If enabled, some light will be lost due to free carrier absorption. If the device has texture, then the photons do not travel parallel to the solution direction (x). The direction they travel makes a different angle with respect to x near the front surface than near the back. Both angles are calculated using the facet angle and the index of refraction for the material of region 1, with the transition between these two angles assumed to occur abruptly when x exceeds one-sixth of the facet depth. If the internal reflectance for the surface opposite the incident surface is non-zero, then some photons reflect from that surface with either the same angle at which they arrived (specular) or randomly-directed (diffuse). If the internal reflectance at the incident surface is non-zero, then some of this reflected light gets trapped within the device until it eventually is either absorbed in the device or fails to be reflected from one surface of the other.

Photogeneration Profile

One photogeneration option is to supply an external ASCII file with suffix ".GEN" that contains photogeneration information. This file should have two values on each line, separated by one or more spaces or by a tab. The first value is a position representing the distance of that location from the front surface, in μm. The second value is the cumulative photogeneration rate in the device between the front surface and that position, in carrier-pairs per second per square cm of projected area. Both the position and photogeneration values must be monotonically increasing functions within the file, and both must start with a value of 0.0 on the first line. Photogeneration information provided for positions beyond the rear surface of the device are ignored. If the device is thicker than the last entry in the file, then no photogeneration is assumed beyond the last position defined in the file.

Primary/Secondary Illumination Intensity

These commands open a dialog box to examine or modify the magnitude and time dependence of light incident on the device, and to select whether the light is incident on the front or rear surface of the device. To use either of the illumination sources, you must first Enable that source from within this dialog box. Different values of illumination source

intensity can be specified for steady state versus transient conditions. Changing the intensity between its steady-state and initial transient value causes a step change in intensity at $t = 0$. Setting the final transient value different from the initial transient value causes the intensity to sweep linearly from the initial to the final value during the course of the transient solution. The values entered correspond to the total power density normally incident on the surface of the device, measured in W/cm². One standard "terrestrial sun" corresponds to an intensity of 0.1 W/cm².

When a simple linear ramp of intensity is inadequate, time-dependent light intensity values can be entered from an external ASCII data file having a filename suffix ".LGT". Each line in the file should contain two values, separated by one or more spaces or by a tab. The first is a time, in seconds. The second is an intensity value with units of W/cm². The lines must have monotonically increasing time values. The maximum number of lines in the file is 1000, (increased from 200 in version 5.9). The time values in this file do not affect the time step size or number of time steps used in the solution. Rather, an intensity value is interpolated from the LGT file for each point in time specified in the Mode command.

Primary/Secondary Illumination Spectrum

The illumination spectrum choices are Monochrome, Black-Body, or External. The Monochrome option allows you to specify that all of the incident power occurs at a single wavelength. Different values of wavelength can be specified for steady state versus transient conditions. Changing the wavelength between its steady-state and initial transient value causes a step change in wavelength at $t = 0$. Setting the final transient value different from the initial transient value causes the wavelength to sweep linearly from the initial to the final value during the course of the transient solution. The Black-Body option allows you to invoke a black-body spectrum corresponding to a specified temperature. The spectrum is actually implemented as a group of discrete wavelengths, so you must declare the number of discrete wavelengths (maximum 1000, increased from 200 in version 5.9) and the range of wavelengths to include. You can artificially limit the wavelength range to simulate the effect of a filtered spectrum. The total power density in the black-body spectrum incident on the device is adjusted to match the values specified for illumination intensity. Note that for a given temperature, there is a limit to the intensity that can be obtained from a black body source; however, PC1Dmod does not verify whether this limit has been exceeded. The External option allows you to supply an external ASCII file that defines a spectral distribution, represented as a group of discrete wavelengths. These files have suffix ".SPC". Several important spectra are provided with PC1Dmod, including the air-mass 1.5 direct and global ASTM solar spectra, and the extraterresrial solar spectrum. These files contain two values on each line, separated by one or more spaces or a tab. The first value is a wavelength in nm, and the second is a power density in W/cm² (NOT spectral density, W/μm/cm²). The entries must be in order of increasing wavelength, with a maximum of 1000 wavelengths allowed (up from 200 in version 5.9). The power densities are scaled as necessary so that the total light intensity for the spectrum as a whole equals the value specified for illumination intensity.

Version 6.2 is distributed along new, default solar spectrum files for AM1.5G, AM1.5D and AM0, with improved resolution and a higher level of detail. The spectra are obtained from the IEC norm [32]. The spectral range of 300 to 4000 nm is evenly sampled in 5 nm wavelength intervals. Note that a finer resolution does not significantly increase the accuracy for typical solar cell setups.

7.5 Compute menu

The Compute menu offers the following commands:

Run	Begins numerical solution of the problem as currently set up, starting with equilibrium and progressing to steady-state or transient conditions as specified by the current Excitation Mode. *A button on the toolbar (running person) provides a quick way to invoke Run.*
Stop	Stops the numerical computation in progress. The computation is allowed to continue for one second after this command is selected. If it has not then converged, the computation is terminated.
Continue	Resumes the numerical computation that was interrupted by the Stop command. Or, if the excitation for a problem has been changed since it converged, PC1Dmod will redo the last solution phase using the current solution as a starting point. You can use this feature to help convergence in many cases.
Single Step	Computes only the next step in the solution. A “step” is defined here as the unit of computation leading to the next display of graphical information. If the Numerical dialog has been set to display plots after every iteration, then this is only one iteration. Otherwise, the computation proceeds until convergence is obtained for equilibrium, steady state, or one time step. *A button on the toolbar (stepping person) provides a quick way to Single Step.*
Start Again	Resets the computation so that a subsequent Single Step command will start with problem initialization and equilibrium solution. Note that the Run command always starts with problem initialization.
Batch	Opens a dialog box for enabling batch mode and identifying which tab-delimited ASCII file contains the batch-parameter information.
Numerical	Opens a dialog box for setting the parameters that control the numerical method. These affect the number of finite elements and the convergence of the solution.

Batch Mode (Compute menu)

Batch mode is a short cut which allows you to rapidly perform an optimization study for a particular configuration (PRM file). Rather than creating a series of PRM files, you only need to create one, and then specify which parameters should be varied. To do a batch run, click the ‘Batch’ button on the toolbar (the icon shows many people running). Parameters can be chosen from the drop-down lists. There’s a description of the parameter at the bottom of the dialog box. For input parameters, you need to specify the range to be varied over, the number of different values, and if they should be varied logarithmically or linearly. When you’ve finished, press OK. The table will appear at the bottom of the parameter view. Results parameters will appear as question marks. Run the simulation as normal. As each result is calculated, it will appear in the table, replacing the question mark. The number of simulations performed so far will be displayed in the title bar.

Examining the results

Use the Copy button to copy the results into the clipboard. From there, they can be pasted into other programs. For example, the results could be pasted into a spreadsheet and graphed. If you’re interested in how a particular graph varies, select it in Interactive Graph View before running the batch. After the batch has finished, use the PageUp and PageDown keys to see how the graphs varied for different parameter values. (You can keep the axes

constant while doing this by selecting 'retain zoom' in the Graph menu. You can reset the graphs using 'reset history graphs' in the same menu). Note: Any parameter that is disabled in the PRM file will have no effect on batch results. For example, the front texture angle is irrelevant if texturing is disabled.

Advanced feature: Permute

If you vary multiple parameters, they can be varied together, or you can solve for all combinations. Click the 'Permute' check box to do all permutations of that input parameter. If permute is off, the parameter will be tied to the parameter above it.

External Batch Files

If you find the 'QuickBatch' method is too restrictive, you can also use an external batch file. This file should contain only the parameters that vary between simulations, and the results that are desired. For example, a batch file for a solar cell could contain a list of background doping values, and V_{oc}, I_{sc} and P_{max} as desired results. To perform a batch run, do the following steps: From a spreadsheet (e.g. Microsoft Excel), enter the parameters in tabular form. Place input parameters on the left hand side of the table, and results parameters on the right. The parameters can be chosen from a list of about 150. (See below for the list). There is no intrinsic limit to the length of a batch file. Previously, batch files were limited to 100 lines. The maximum number of lines now depends on the operating system you are using. In Windows 95, batch files are limited to a few hundred lines (more if smaller font sizes are used in Parameter View). This limitation doesn't apply to Windows NT. Batch files can have 30 fields across (although only the first 12 will print on A4 paper, unless you select a very small font size or copy the results into a spreadsheet program). Save the table in "Tabbed Text" format. The file should end in ".txt".

From PC1Dmod, open your PRM file. Using the Compute:Batch menu, select the text file that you created with your spreadsheet. Note: Shortcuts to files on network drives are not supported. You must select the batch file directly.

For a list of all batch parameters and help setting up a suitable batch file, see the PC1D batch file generator, at
https://www2.pvlighthouse.com.au/Resources/PC1D/PC1D%20Batch%20File%20Generator.aspx

Numerical Command (Compute menu)

This command opens a dialog box which allows you to set the following parameters which affect the numerical computation algorithm. These parameters do not alter the definition of either the device or the excitation, but they will influence the accuracy of the solution and the speed with which the solution converges to an answer. Improper settings of these parameters can cause the program to fail to converge even for simple problems, so the default values of each parameter are listed here for reference.

Element Size Factor	This value determines the size of the finite elements used to partition the device. A smaller element size factor produces smaller elements, which improves accuracy but takes more time. The default value is 0.5. Values greater than 1.0 can produce elements so large that convergence problems may arise. Once the factor is small enough that all 500 available elements are used, making it smaller will have no further effect.
Normalized Error Limit	This value determines when the solution is said to have converged. Iterations will continue until the largest change in any of the three potentials (electron or hole quasi-Fermi potential, or electrostatic potential) at any node is less than this factor times the thermal voltage, *kT/q* (which is about 26 mV at room temperature). The

default value is 1E-6, and will rarely need modification.

Normalized Potential Clamp	This value determines the maximum change in one iteration that is allowed for any potential at any node, as a multiple of the thermal voltage, *kT/q*. The default value is 1, which is rather conservative, favoring robustness over speed. Increase this value for more speed if convergence is not a problem. In particular, a higher value may be desirable to increase speed when large reverse-bias voltages are imposed. Note that you can change the clamp value during a solution, for those times when you need a small value for steady state but a larger value will do for subsequent transient steps.
Clamping Phi/Psi	These check boxes determine how the Normalized Potential Clamp is imposed. Selecting Psi clamping prevents the electrostatic potential from changing by more than the clamp amount with each iteration. Selecting Phi prevents the separation between each quasi-Fermi potential and the electrostatic potential from changing too much. AT LEAST ONE OF THESE BOXES SHOULD BE SELECTED, as many problems will "blow up" very quickly without some form of clamping imposed. The default is for both boxes to be selected.
Maximum Time	This value determines how long (in seconds) a solution is permitted to continue before it is judged to be non-convergent. The default value is 60 seconds. Some problems involving internal shunt elements may take longer than this to converge, but most problems that haven't converged after a minute never will.
Renode	These three check boxes determine when the finite-element nodes are reallocated. When initialized, the problem has 100 elements in each defined region. It is usually desirable to renode during the equilibrium solution, since the initial node allocation does not yet know where the critical junction regions are located. Selecting renode for the steady-state solution serves to refine the previous node allocation based on the equilibrium solution, and allows the program to do an emergency renode if the quasi-Fermi potential step across any one element exceeds 32 times the thermal voltage. Renoding for a transient solution should only be invoked when the excitation significantly alters the space-charge regions, and it should especially be avoided during fast transients where time derivatives are important. The default is to renode during equilibrium and steady state solutions, but not during transient solutions.
Display graphs after every iteration	This check box is provided for those who are interested in observing the numerical computation performed by PC1Dmod. When checked, the plots on screen are updated after every iteration, not just when the solution has converged. This slows the solution considerably, so should be chosen only when the convergence behavior is of interest.
Total velocity saturation	This check box is provided for those who need to impose rigid saturation of the total velocity of the carriers, due to both drift and diffusion. Normally, when this box is not selected, the mobility of the carriers is reduced only in response to a high electric field. When this box is selected, the mobility is reduced in response to a high gradient in the quasi-Fermi potential. Although checking this box invokes the more-correct physical limitation, convergence is more difficult and solutions can take more than twice as long to complete. It is recommended only for heterostructure devices in which the current is

limited by thermionic emission over an energy barrier.

7.6 Graph menu

The Graph menu provides commands that control which graph is available for inspection using the Interactive-Graph view. It also provides a command for resetting the graphs in the Four-Graph view to their default values, and a command for copying data to the Windows clipboard.

Spatial Graphs	This selection provides a menu of choices for interactive graphs that display spatial information (functions of position). If the information you seek is not included in this list, many more functions are available for a Defined Graph.
Temporal Graphs	This selection provides a menu of choices for interactive graphs that display temporal information (functions of time). Some functions not included in this list can be accessed for a Defined Graph.
Defined Graph	This selection opens a dialog box which allows you to specify x and y functions for any graph, selected from 75 available functions. These functions provide a much more detailed look at the operation of the device than is available from the predefined graphs.
Auxiliary Graph	This command opens a dialog box for selecting a spatial function and a position within the device. Once this information has been entered, any subsequent transient solutions will store the value of that function at that position as a function of time. The data can then be viewed as using the Auxiliary selection from the Temporal Graph menu.
Experimental	This command opens a dialog box for selecting data from an external file. The data can be viewed on a user-defined graph with “Experimental Data” as one of the data types. The experimental data file should be a tab-delimited text file. No unit conversion is performed on this data – it’s your responsibility to ensure that the data is sensible.
Default Graphs	This command is only active in Four-Graph view, in which case it resets the four graphs to the default selections. When graphs are chosen for interactive examination, they are added to the four-graph view, displacing the default graphs that were there initially. This is done to make it easy to return to those graphs, by double-clicking on them in the Four-Graph view. However, if your attention shifts to a new issue, you will likely want to restore the default graphs, which are chosen to provide a balanced overview of the device's operation.
Previous History Graph, Next History Graph	Whenever a simulation is completed, the current interactive graph is saved (to a maximum of 100 graphs). You can view these ‘history’ graphs using the Graph menu or the Page Up/Page Down keys. By flipping through these graphs, you can visually compare

	simulation results. This feature is especially useful for batch runs.
Retain zoom for history graphs	If this is OFF, the previous (history) graphs will be auto-scaled, so that they are fully visible. Unfortunately, this means that the axes can change, making it hard to compare different results. If Retain Zoom is ON, the axes will not change. You can zoom into a part of the curve, then see how that portion differs from other simulation results. You can zoom out to see the full graph.
Reset history graphs	Removes all the accumulated history graphs, allowing you to start afresh.
Copy Data	This command for copying data to the Windows clipboard for export to other programs is enabled in two situations. First, it is enabled for the Interactive-Graph view, in which case this command copies the data that is currently displayed on the graph. Second, it is enabled in Parameter view if Batch Mode is being used, in which case this command copies the data from the batch table to the clipboard.

This is the view you will want to use most often when inspecting solution results. It displays a single graph, and allows you to zoom into regions of the graph, and extract the values of individual points.

To zoom into part of the graph:

With the mouse: Press the left mouse button. Drag over the area you want to zoom into. Release the left mouse button. (To cancel the zoom, press the right mouse button or the ESC key).

With the keyboard: Use the arrow keys to move the caret (the blinking line) to one end of the area you are interested in. Press ENTER. Move the caret to the other end. Press ENTER.

To zoom out:

With the mouse: Press the right mouse button.

With the keyboard: Press the ESC key.

Zooming out when the graph is already fully 'zoomed out' will return you to the four-graphs view.

To examine graphs from previous simulations:

Press PAGEUP or PAGEDOWN to view the graphs from the last 16 simulations.

7.7 View menu

The View menu offers the following commands:

Toolbar

Shows or hides the toolbar.

Use this command to display and hide the Toolbar, which includes buttons for some of the most common commands in PC1Dmod, such as File Open. A check mark appears next to the menu item when the Toolbar is displayed.

The toolbar is displayed across the top of the application window, below the menu bar. The toolbar provides quick mouse access to many tools used in PC1Dmod.

To hide or display the Toolbar, choose Toolbar from the View menu (ALT, V, T).

For help on the use of a particular toolbar button, select the button at the far right edge of the toolbar, displaying a question mark and an arrow. The cursor will change to match this button. Point the new cursor to the button in question and press the mouse key. A Help file will open on-screen with information about the purpose of that button.

Status bar

Shows or hides the status bar.
Use this command to display and hide the Status Bar, which describes the action to be executed by the selected menu item or depressed toolbar button, and keyboard latch state. A check mark appears next to the menu item when the Status Bar is displayed.
The status bar is displayed at the bottom of the PC1Dmod window. To display or hide the status bar, use the Status Bar command in the View menu.
The left area of the status bar describes actions of menu items as you use the arrow keys to navigate through menus. This area similarly shows messages that describe the actions of toolbar buttons as you depress them, before releasing them. If after viewing the description of the toolbar button command you wish not to execute the command, then release the mouse button while the pointer is off the toolbar button.
The right areas of the status bar indicate the following:

Indicator	Description
Iteration Counter	During a numerical solution, this frame shows how many iterations have been completed toward the current solution.
Convergence Indicator / Element Counter	During a numerical solution, this frame shows a bar that moves towards the right as the numerical solution converges to an answer. Otherwise, this frame indicates how many finite elements are defined for the device.
Solution Status	This field indicates the status of the current numerical solution. If blank, then the current problem has not yet been solved, or the parameters have been changed since the last solution. Valid solutions are indicated as Equil, Steady, or Trans for Equilibrium, Steady-State, or Transient results. Do not use displayed results unless the Status frame indicates a valid solution.
Time Step Number	During a transient solution, this frame shows for which time step number the displayed graphs apply.

Parameter view

The Parameter view is the start-up default. This text-type screen lists all of the parameters that define your problem, and at the end there is a section for reporting the results of calculations. You can double-click the mouse on most lines in the Parameter view to open a dialog box to modify that parameter.
A schematic diagram of the device is also displayed, providing visual feedback of doping, texturing, and internal shunt elements. This makes it easier to recognize mistakes when designing complex devices. You can also double-click on parts of the diagram to change various parameters.

Four-graph view

The Four-Graph view provides a quick overview of what's happening in your device. Double click on any of the four graphs to select it for detailed examination using the Interactive-Graph view.

Interactive-graph view

The Interactive Graph view allows you to examine specific data values on a graph. If the data you need is not in one of the predefined graphs, you can create a user-defined graph using the Graph menu to access any of 55 different functions.

7.8 Options menu

The Options menu provides commands that affect the environment in which PC1Dmod runs on your computer, but which have no effect whatever on the problem or its solution. The features you select with these commands are stored on your computer in a file named PC1D.INI which is normally stored in your WINDOWS directory. Consequently, they will be used whenever you start PC1Dmod on your computer. They will not apply if you save a problem file on disk and subsequently work with it using a different computer.

File Locations — This command opens a dialog box which allows you to specify which subdirectory you would like to serve as the default location for each type of external file used by PC1Dmod. By segregating your files into separate directories, you will find it much easier to locate the files that you need later. If a field is left blank, the default location is assumed to be the directory from which PC1Dmod was started.

Store Node Data — This command, when ticked, instructs PC1Dmod to store the current solution on disk whenever it stores the current problem parameters. This is useful if you are in the middle of examining a solution in detail but need to quit the program for a period. Saving the node data preserves the most recent solution details, preventing you from needing to repeat the solution when you return, but it also increases the size of the saved PRM files substantially. The default is for this option to be disabled.

Device Update — This command, when ticked, instructs PC1Dmod to update all of the on-screen graphs whenever a change is made in any of the parameters that define the device. This can be quite helpful when setting up the device parameters, because you can immediately see the impact of a change in doping, thickness, etc. The default for this option is for it to be enabled. However, some computers may not be fast enough to keep up. If your computer seems to be lagging behind you when you are setting up a problem, consider disabling this option.

7.9 Help menu

The Help menu offers the following commands, which provide you assistance with this application:

- User Guide — Directs you to this user guide
- About — Displays the version number of this application.

7.10 Advanced output options

PC1Dmod 6.2 also has included some new options for the program outputs in the result section, in the graph view and in batch mode.
Firstly, the main current-voltage curve parameters which are commonly calculated by many PC1D users manually are now directly accessible, including the short-circuit current density, the fill factor, the current and voltage at the maximum power point and the maximum power density.
Secondly, there is a possibility to directly output the saturation current density $J_{0\mathrm{e}}$ at *pn* junctions. The emitter simulation results ($J_{0\mathrm{e}}$, sheet resistance ρ_{sheet} and junction depth x_j) are available when using a specific excitation file, which sets the junction under a moderate forward bias of 0.55 V in the dark. For a p-type substrate, $J_{0\mathrm{e}}$ is then calculated from the hole recombination current density J_p at a depth x_e using the same procedure used in the dedicated emitter recombination tool EDNA 2 [33]:

$$J_{0\mathrm{e}} = \frac{J_p(x_e)}{n(x_e) \cdot p(x_e) - n_{\mathrm{i,eff}}^2(x_e)} n_{\mathrm{i,eff}}^2(x_e). \tag{59}$$

Here, $n_{\mathrm{i,eff}}$ is the effective intrinsic carrier density (including BGN) and x_e is the depth corresponding to the edge of the emitter side of the space charge region, taken as the point where $n_0(x_e) = 10 \times N_A$, where N_A is the acceptor base doping.
Finally, because PC1Dmod has the ability to perform transient simulations, it is also suited for simulating injection-dependent lifetime characteristics that can be measured using the quasi steady state photoconductance (QSSPC) technique, another important topic for Si solar cell research and development. In PC1Dmod 6.2, this simulation is coded into the program in such a way that the user is able to directly output the effective carrier lifetime as a function of the excess minority carrier density for a given lifetime sample. These calculations are also used together with a dedicated excitation file setting up the transient lifetime measurement, with secondary files specifying the light pulse and the flash spectrum. Note that when SRH recombination is disabled both for the surfaces and the bulk of the wafer the result corresponds to the intrinsic recombination curve of the Si material. With this functionality, PC1Dmod 6.2 offers the possibility to not only calculate the injection-dependent Auger lifetime or SRH lifetime, but also a combination of Auger, radiative, bulk SRH and surface SRH including the effect of surface charges and the depth-dependent variations of the carrier densities.

8 Physical constants

The following physical constants are used in PC1Dmod calculations.

Name	Symbol	Value
Elementary charge	q	$1.602176565\times10^{-19}$ C
Thermal voltage at 300 K	kT/q	0.025851992 V
Photon energy factor	$h\cdot c$	1239.84193 eV·nm
Permittivity of free space	ε_0	8.8541878×10^{-14} F/cm
Kelvin-Celsius offset		273.15 K
Circle geometry constant	π	3.14159265359

(http://physics.nist.gov/cuu/Constants/index.html, March 2015)

The following program constants are constraints in this version of PC1Dmod:

Parameter	Maximum	
No. of Elements	5000	(up from 500)
No. of Time Steps	1000	(up from 200)
No. of Wavelengths	1000	(up from 200)
No. of Regions	5	
No. of Batch Columns	30	
No. of Lines of External Files	1000	(up from 200)

9 Bibliography

9.1 PC1Dmod program development

- H. Haug, and J. Greulich, “PC1Dmod 6.2 – Improved simulation of c-Si devices with updates on device physics and user interface,” *Energy Procedia*, submitted for publication, 2016.
- H. Haug, J. Greulich, A. Kimmerle, and E.S. Marstein, “PC1Dmod 6.1 - state-of-the-art models in a well-known interface for improved simulation of Si solar cells,” *Solar Energy Materials and Solar Cells*, vol. 142, pp. 47-53, 2015.
- H. Haug, A. Kimmerle, J. Greulich, A. Wolf and E.S. Marstein, "Implementation of Fermi-Dirac statistics and advanced models in PC1D for precise simulations of silicon solar cells," *Solar Energy Materials and Solar Cells*, vol. 131, pp. 30-36, 2014.
- H. Haug, B. R. Olaisen, Ø. Nordseth and E. S. Marstein, "A graphical user interface for multivariable analysis of silicon solar cells using scripted PC1D simulations," *Energy Procedia*, **38**, pp. 72–79, 2013.
- Clugston, D.A. and Basore, P.A., “PC1D Version 5: 32-bit Solar Cell Simulation on Personal Computers,” 26th IEEE Photovoltaic Specialists Conf. (Sept 1997).
- Basore, P.A. and Clugston, D.A., “PC1D Version 4 for Windows: From Analysis to Design,” 25th IEEE Photovoltaic Specialists Conf., (May 1996).
- Basore, P.A., "PC-1D Version 3: Improved Speed and Convergence," 22nd IEEE Photovoltaic Specialists Conf., (October 1991).
- Basore, Rover, and Smith, "PC-1D Version 2: Enhanced Numerical Solar Cell Modeling," 20th IEEE Photovoltaic Specialists Conf., (September 1988).
- Rover, Basore, and Thorson, "Solar Cell Modeling on Personal Computers," 18th IEEE Photovoltaic Specialists Conf., Las Vegas (October 1985).

9.2 Physical models included in PC1D version 5.9

- Adachi, J. Appl. Phys. 58, p. 1 (1985). (GaAs, AlGaAs electronic properties)
- Arora, Hauser, and Roulston, IEEE Trans. on Electron Devices ED-29(2), p. 292 (February 1982). (Silicon transport properties)
- Aspnes, Kelso, Logan, and Bhat, J. Appl. Phys. 60, p. 754 (1986). (GaAs, AlGaAs optical properties)
- Aspnes and Studna, Physical Review B 27, p. 985 (1983). (InP, Ge optical properties)
- ASTM Standard E891-R4, Annual Book of ASTM Standards (1985) (AM1.5 Direct Spectrum)
- ASTM Standard E892-R4, Annual Book of ASTM Standards (1985) (AM1.5 Global Spectrum)
- Camassel and Auvergne, Phys. Rev. B 12, p. 3258 (1975). (Ge electronic properties)
- Camassel, Auvergne, and Mathieu, J. Appl. Phys. 46, p. 2683 (1975). (GaAs electronic properties)

- Del Alamo, Swirhun, and Swanson, Solid-State Electronics 28 (1-2), p. 47 (1985). (Silicon transport and recombination properties)
- Fan, Y.H., “Semiconductors and Semimetals”, ed. R.K. Williamson and A.C. Beer, Academic Press (1967), Vol 3, p.409. (III-V free-carrier absorption)
- Fonash, J., Solar Cell Device Physics, Academic Press, N.Y.(1981). (Ge electronic properties)
- Haas, J. Phys. Chem. Solids 23, p. 821 (1962). (Ge optical properties)
- Haug, J. Phys. C: Solid State Phys. 16, p. 4159 (1983). (GaAs, AlGaAs recombination coefficients)
- Hurkx, Klaassen, and Knuvers, “A New Recombination Model for Device Simulation Including Tunneling”, IEEE Trans. Electron Devices, ED-39, (Feb. 1992), pp. 331-338. (Field-enhanced recombination).
- Karpova and Kalashvikov, Proceedings of the International Conference on the Physics of Semiconductors, p. 880 (1962) (Ge recombination coefficients)
- Klausmeier-Brown, Lundstrom, and Melloch, Appl Phys. Lett. 52 (26), p. 2255 (June 1988). (GaAs electronic properties)
- McLean, T.P., Progress in Semiconductors, Vol. 5, Heywood, London (1960). (Ge electronic properties)
- Morin, Phys. Rev. 94, p. 1525 (1954). (Ge transport properties)
- Prince, Phys. Rev. 92, p. 681 (1953). (Ge transport properties)
- Rajkanan, Singh, and Shewchun, Solid-State Electronics 22, p. 793 (1979). (Silicon optical properties)
- Schlangenotto, Maeder, and Gerlach, “Temperature Dependence of the Radiative Recombination Coefficient in Silicon”, Physica Status Solidi A21, 357-367 (1974). (Silicon recombination)
- Schroder, Thomas, and Swartz, “Free Carrier Absorption in Silicon”, IEEE Trans. Electron Devices, ED-25, (Feb. 1978), pp. 254-261. (Si free-carrier absorption)
- Sigai, Abrahams, and Blanc, J. Electrochem. Soc 119, p. 952 (1972). (AlGaAs transport properties)
- Sproul, Green, and Zhao, Appl. Phys. Lett. 57 (3), p. 255 (July 1990). (Intrinsic concentration in silicon).
- Swanson and Swirhun, "Characterization of Majority and Minority Carrier Transport in Heavily Doped Silicon," Sandia National Laboratories contractor report, SAND87-7019 (November 1987). (Silicon transport and recombination properties).
- Sze, S., Physics of Semiconductor Devices, 2nd. Ed., J. Wiley and Sons, New York, 1981, p. 850. (Si electronic properties)
- Takeshima, J. Appl. Phys. 58, p. 3846 (1985). (AlGaAs recombination coefficients)
- Takeshima, Jap. J. Appl. Phys. 22, p. 491 (1983) (InP recombination coefficients)
- Thekaekara, Solar Energy Engineering, Ed. by A.A.M. Sayigh, Academic Press, New York, 1977, p. 40. (AM0 Spectrum)
- Thurber, Mattis, Liu, and Filliben, “The Relationship Between Resistivity and Dopant Density for Phosphorus- and Boron-Doped Silicon,” U.S. Department of Commerce National Bureau of Standards, (1981). (Si majority carrier mobilities)
- Thurmond, J. Electrochemical Soc. 122, p. 1133 (1975). (Si, GaAs, Ge optical properties)
- Turner, Reese, and Pettit, Phys. Rev. A 136, p. 1467 (1964) (InP electronic properties)
- Tyler and Woodbury, Phys. Rev. 102, p. 647 (1956). (Ge transport properties)
- Vilms and Garrett, Solid State Electron. 15, p. 443 (1972). (GaAs transport properties)
- Walukiewicz, et. al., J. Appl. Phys. 51, p. 2659 (1980). (InP transport properties)
- Wang, Misiakos, and Neugroschel, IEEE Trans. on Electron Devices ED-37 (5), May 1990, p. 1314. (Silicon minority hole mobility).

- Wiley, J., Semiconductors and Semimetals, Vol. 10, Academic Press, N.Y. (1975). (InP, GaAs, AlGaAs transport properties)
- Yahia, Wanlass, and Coutts, 20th IEEE Photovoltaic Specialists Conf. (September 1988) (InP recombination coefficients)

9.3 Numerical method included in PC1D version 5.9

- Basore, P.A. "Numerical Modeling of Textured Silicon Solar Cells Using PC-1D," IEEE Trans. on Electron Devices, ED-37 (2), (February 1990).
- Basore, P.A., "Essential Elements in the Numerical Modeling of Solar Cells," 4th Photovoltaic Science and Engineering Conf., (February 1989).
- Grossman and Hargrove, "Numerical Solution of the Semiconductor Transport Equations with Current Boundary Conditions," IEEE Trans. on Electron Devices ED-30 (9), pp. 1092-1096 (September 1983).
- Dongarra, Moler, Bunch, and Stewart, LINPACK User's Guide, SIAM, Philadelphia (1979).
- Lundstrom, Schwartz, and Gray, "Transport Equations for the Analysis of Heavily Doped Semiconductor Devices," Solid-State Electronics 24, pp. 195-202.
- Lundstrom and Schuelke, "Numerical Analysis of Heterostructure Semiconductor Devices," IEEE Trans. on Electron Devices ED-30 (9), pp. 1151-1158 (September 1983).
- Mock, Analysis of Mathematical Models of Semiconductor Devices, Boole Press, Dublin.
- Selberherr, Analysis and Simulation of Semiconductor Devices, Springer-Verlag, New York.
- Sutherland and Hauser, "A Computer Analysis of Heterojunction and Graded Composition Solar Cells," IEEE Trans. on Electron Devices ED-24, pp. 363-372 (1972).
- Thorson, G.M., "A Solar Cell Simulator for Personal Computers," M.S. Thesis, Iowa State University, Ames, IA, 1985.

9.4 References added for cmd-PC1D and PC1Dmod

[1] P. P. Altermatt, A. Schenk, F. Geelhaar, and G. Heiser, "Reassessment of the intrinsic carrier density in crystalline silicon in view of band-gap narrowing," *Journal of Applied Physics,* vol. 93, pp. 1598-604, 2003.

[2] M. A. Green, "Intrinsic concentration, effective densities of states, and effective mass in silicon," *Journal of Applied Physics,* vol. 67, pp. 2944-54, 1990.

[3] A. Schenk, "Finite-temperature full random-phase approximation model of band gap narrowing for silicon device simulation," *Journal of Applied Physics,* vol. 84, pp. 3684-95, 1998.

[4] D. Yan and A. Cuevas, "Empirical determination of the energy band gap narrowing in highly doped n+ silicon," *Journal of Applied Physics,* vol. 114, p. 044508, 2013.

[5] D. Yan and A. Cuevas, "Empirical determination of the energy band gap narrowing in p^+ silicon heavily doped with boron," *Journal of Applied Physics,* vol. 116, p. 194505, 2014.

[6] D. B. M. Klaassen, "A unified mobility model for device simulation - I. Model equations and concentration dependence," *Solid-State Electronics,* vol. 35, pp. 953-9, 1992.

[7] D. B. M. Klaassen, "A unified mobility model for device simulation - II. Temperature dependence of carrier mobility and lifetime. ," *Solid State Electronics,* vol. 35, pp. 961-7, 1992.

[8] F. Schindler, M. Forster, J. Broisch, J. Schön, J. Giesecke, S. Rein*, et al.*, "Towards a unified low-field model for carrier mobilities in crystalline silicon," *Solar Energy Materials and Solar Cells,* vol. 131, pp. 92-99, 2014.

[9] A. Richter, S. W. Glunz, F. Werner, J. Schmidt, and A. Cuevas, "Improved quantitative description of Auger recombination in crystalline silicon," *Physical Review B,* vol. 86, pp. 1-14, 2012.

[10] M. J. Kerr and A. Cuevas, "General parameterization of Auger recombination in crystalline silicon," *Journal of Applied Physics,* vol. 91, pp. 2473-80, 2002.

[11] P. P. Altermatt, A. Schenk, and G. Heiser, "A simulation model for the density of states and for incomplete ionization in crystalline silicon. I. Establishing the model in Si : P," *Journal of Applied Physics,* vol. 100, p. 113714, 2006.

[12] P. P. Altermatt, A. Schenk, B. Schmithusen, and G. Heiser, "A simulation model for the density of states and for incomplete ionization in crystalline silicon. II. Investigation of Si : As and Si : B and usage in device simulation," *Journal of Applied Physics,* vol. 100, p. 113715, Dec 1 2006.

[13] H. Steinkemper, M. Rauer, P. Altermatt, F. D. Heinz, C. Schmiga, and M. Hermle, "Adapted parameterization of incomplete ionization in aluminum-doped silicon and impact on numerical device simulation," *Journal of Applied Physics,* vol. 117, p. 074504, 2015.

[14] M. Forster, A. Cuevas, E. Fourmond, F. E. Rougieux, and M. Lemiti, "Impact of incomplete ionization of dopants on the electrical properties of compensated p-type silicon," *Journal of Applied Physics,* vol. 111, p. 043701, 2012.

[15] A. Kimmerle, M. M. Rahman, S. Werner, S. Mack, A. Wolf, A. Richter*, et al.*, "Precise parameterization of the recombination velocity at passivated phosphorus doped surfaces," *Journal of Applied Physics,* vol. 119, p. 025706, 2016.

[16] M. A. Green, "Self-consistent optical parameters of intrinsic silicon at 300 K including temperature coefficients," *Solar Energy Materials & Solar Cells,* vol. 92, pp. 1305-10, 2008.

[17] H. Fan, O. Willardson, and O. Beer, "Semiconductors and semimetals," ed: ed. RK Williamson and AC Beer, Academic Press, 1967, p. 409.

[18] M. Rüdiger, J. Greulich, A. Richter, and M. Hermle, "Parameterization of free carrier absorption in highly doped silicon for solar cells," *IEEE Transactions on Electron Devices,* vol. 60, pp. 2156-63, 2013.

[19] S. C. Baker-Finch, K. R. McIntosh, D. Yan, K. C. Fong, and T. C. Kho, "Near-infrared free carrier absorption in heavily doped silicon," *Journal of Applied Physics,* vol. 116, p. 063106, 2014.

[20] P. E. Schmid, "Optical absorption in heavily doped silicon," *Physical Review B (Condensed Matter),* vol. 23, pp. 5531-6, 1981.

[21] M. A. Green, *Silicon solar cells: advanced principles and practice*. Sydney, Australia: Centre for Photovoltaic Devises and Systems UNSW, 1995.

[22] P. A. Basore, "Numerical modeling of textured silicon solar cells using PC-1D," in *Proceedings of the 21st IEEE Photovoltaic Specialists Conference*, Kissimmee, FA, USA, 1990, pp. 337-43.

[23] P. A. Basore, "Extended spectral analysis of internal quantum efficiency," in *Proceedings of the 23rd IEEE Photovoltaic Specialists Conference*, Louisville, Kentucky, USA, 1993, pp. 147-52.

[24] J. A. del Alamo and R. M. Swanson, "The physics and modeling of heavily doped emitters," *IEEE Transactions on Electron Devices,* vol. ED-31, pp. 1878-88, 1984.

[25] D. M. Caughey and R. E. Thomas, "Carrier mobilities in silicon empirically related to doping and field," *Proceedings of the IEEE,* vol. 55, pp. 2192-3, 1967.

[26] N. D. Arora, J. R. Hauser, and D. J. Roulston, "Electron and hole mobilities in silicon as a function of concentration and temperature," *IEEE Transactions on Electron Devices,* vol. ED-29, pp. 292-5, 1982.

[27] P. P. Altermatt, F. Geelhaar, T. Trupke, X. Dai, A. Neisser, and E. Daub, "Injection dependence of spontaneous radiative recombination in c-Si: experiment, theoretical analysis, and simulation," in *Proceedings of the 5th International Conference on Numerical Simulation of Optoelectronic Devices*, Berlin, Germany, 2005, pp. 47-8.

[28] G. A. M. Hurkx, D. B. M. Klaassen, and M. P. G. Knuvers, "A new recombination model for device simulation including tunneling," *IEEE Transactions on Electron Devices,* vol. 39, pp. 331-8, 1992.

[29] P. P. Altermatt, J. O. Schumacher, A. Cuevas, S. W. Glunz, R. R. King, G. Heiser*, et al.*, "Numerical modeling of highly doped Si:P emitters based on Fermi-Dirac statistics and self-consistent material parameters," *Journal of Applied Physics,* vol. 92, pp. 3187-97, 2002.

[30] Y. Chen, H. Shen, and P. P. Altermatt, "Analysis of recombination losses in screen-printed aluminum-alloyed back surface fields of silicon solar cells by numerical device simulation," *Solar Energy Materials and Solar Cells,* vol. 120, pp. 356-362, 2014.

[31] H. Haug, A. Kimmerle, J. Greulich, A. Wolf, and E. S. Marstein, "Implementation of Fermi–Dirac statistics and advanced models in PC1D for precise simulations of silicon solar cells," *Solar Energy Materials and Solar Cells,* vol. 131, pp. 30-6, 2014.

[32] IEC, *Photovoltaic devices - part 3: measurement principles for terrestrial photovoltaic (PV) solar devices with reference spectral irradiance data.* , 2nd ed.: International Electrotechnical Commission, 2008.

[33] K. R. McIntosh and P. P. Altermatt, "A freeware 1d emitter model for silicon solar cells," in *Proceedings of the 35th IEEE Photovoltaic Specialists Conference*, Honolulu, Hawaii, USA, 2010, pp. 1-6.